Master's Thesis

Optimization of cell unroofing and *in vitro* reconstitution of reticular adhesion

Mohammed Mostafa Al Quadir

University of Jyväskylä

Department of Biological and Environmental Science

24 May 2024

UNIVERSITY OF JYVÄSKYLÄ, Faculty of Mathematics and Science
Department of Biological and Environmental Science
Master's Degree Programme in Nanoscience

Quadir, Mohammed Mostafa Al Optimization of cell unroofing and *in vitro* re-constitution of reticular adhesion

MSci Thesis 42 p., 2 appendices

Supervisors: Assistant Professor Leonardo Cesar de Almeida Souza, University of Helsinki
And
Professor Janne Ihalainen, University of Jyväskylä

Tarkastajat:

May 2024

Keywords: adhesion, membrane sheets

Reticular adhesions (RAs) are a novel type of cell-ECM adhesion, characterized by the presence of integrin αVβ5 and colocalized with flat clathrin lattices (FCLs) and lack many focal adhesion (FA) components. A distinctive feature of RAs is their persistence during the cytoskeletal changes that occur in cell division, unlike other cell adhesions that typically disassemble. The formation of RAs involves the clustering of integrin αVβ5 and the formation of FCLs, which have been found to be interdependent events. A deeper understanding of why this occurs and what physiological factors trigger RA formation is needed. The *in vitro* reconstitution of RAs is crucial for studying these questions in a controlled manner. This thesis aimed to optimize a method for isolating membrane sheets attached to a solid substrate. It compared two cell unroofing methods, which remove the top membrane and cytosol, leaving the bottom membrane on a solid surface: squashing-peeling and ultrasonication. It also attempted to reconstitute RAs on these membrane sheets and visualize them using TIRF microscopy. This experiment was successful in producing high-quality membrane sheets and in reconstituting RAs on these sheets. Among the two methods employed for generating the membrane sheets, ultrasonication was found to be more effective than the squashing-peeling method for isolating high-quality membrane sheets. The research also indicated that RA formation is temperature-sensitive, with 37°C being the optimal temperature. *In vitro* reconstitution of reticular adhesions presents a powerful approach to studying these novel structures.

TABLE OF CONTENTS

TERMS AND ABBREVIATIONS

Terms

Cell unroofing	Exposing the cytoplasmic side of the cell membrane
Unroofing yield	Percentage of cells successfully unroofed
Reconstitution	Recreating biological systems experimentally
Cell adhesion	Cells binding to extracellular matrix
Adhesion complex	Integrin-based adhesion framework
Adhesome	Adhesion complex protein collective
Consensus adhesome	Adhesion complex intrinsic proteins
Endocytosis	Cellular process engulfing molecules

Abbreviations

RA	reticular adhesion
ECM	extracellular matrix
CME	clathrin-mediated endocytosis
CCS	clathrin-coated structure
FAK	focal adhesion kinase
p-FAK	phosphorylated focal adhesion kinase
TIRF	total internal reflection fluorescence
FA	focal adhesion
FX	focal complex
FB	fibrillar adhesion
NA	nascent adhesion
FN	fibronectin
FCL	flat clathrin lattice
CCP	clathrin-coated pit
AP-2	adaptor protein complex 2
AP-2- σ	adaptor protein complex 2 subunit sigma
WGA	wheat germ agglutinin
DAPI	4',6-diamidino-2-phenylindole
CFP	cyan fluorescent protein
PEI	polyethyleneimine

1 INTRODUCTION

Cells attach and interact with the surrounding extracellular matrix (ECM). This interaction offers structural support, facilitates biochemical signaling, provides mechanical cues, regulates cell dynamics, creates a niche microenvironment, enables tissue differentiation, and embryonic development, and influences disease biology (Ruoslahti *et al.* 1985; Getzoff *et al.* 1987; Morgan *et al.* 2007; Berrier and Yamada 2007; Lock *et al.* 2008; Kanchanawong and Calderwood 2023). Thus, it is crucial for the survival and function of multicellular organisms (Berrier and Yamada 2007). The ECM in living tissues is a three-dimensional dynamic supramolecular complex that encases the majority of cells (Ruoslahti *et al.* 1985). It is mainly made up of water, proteoglycans, and fibrous proteins. These fibrous proteins include collagens, elastins, fibronectins, laminins, etc. (Frantz *et al.* 2010). The ECM in two-dimensional *in vitro* cell culture is much more simplified and is commonly a flat substrate coated with a single or multiple ECM protein(s). This simplified ECM enables controlled studies of cells. Three-dimensional cell culture models, including spheroids and organoids, possess ECMs that more closely resemble those in living organisms (Duval *et al.* 2017). Cells attach to ECM forms by establishing mechanical connections. These connections are made up of multilayered protein structures which are known as adhesion complexes (Abercrombie and Dunn 1975). Among these complexes, those based on integrins have been extensively researched (Chastney *et al.* 2021). Recently, reticular adhesion has emerged as a novel member of the established array of integrin-based adhesion complexes (Lock *et al.* 2018).

1.1 Integrins

Several cell surface receptors like integrins, syndecans, proteoglycans, and cadherins contribute to cell-ECM adhesion. However, integrins are the most studied cell-ECM adhesion receptor because of their versatility, ability to bind to various ECM proteins, and involvement in bidirectional signaling (Hynes 2002). They are transmembrane proteins made of two subunits, alpha (α) and beta (β). In mammals, there are 18 α and 8 β subunits. They pair up in different combinations to form 24 distinct heterodimers. These heterodimers can bind to specific sites within the ECM (Hynes 2002). Once this connection is made, these integrins connect to the cytoskeleton with the help of some intermediate cytoskeleton adaptor proteins such as talin, vinculin, kindlin, paxillin, and focal adhesion kinase (Chastney *et al.* 2021). These molecules interact with the cytoplasmic domains of integrins and increase integrin affinity for ECM ligands (Bachir *et al.* 2014; Li *et al.* 2020). The αβ1-integrin heterodimers are the most common type of integrins that bind to the ECM. They have a specific affinity for ECM components like collagen, laminin, or fibronectin (Chastney *et al.* 2021). On the other hand, the αvβ-integrin family is known for its ability to recognize and bind to the RGD sequence. This sequence is a short chain of three amino acids—arginine (R), glycine (G), and aspartic acid (D)—that is found in many ECM proteins (Akiyama and Yamada 1985).

1.2 Integrin-based cell-ECM adhesions

Integrin-based adhesion complexes are very well studied. They have a distinctive ability to link the ECM to the cell cytoskeleton and react to mechanical stimuli (Kanchanawong and Calderwood 2023). Depending on the maturity stage, function, location, cell cycle, and composition, they can be classified into different types (Table 1).

Table 1: Some of the most common types of integrin-based adhesion complexes with their characteristics.

Type	Associated Integrins	Size	Shape	Location	Associated proteins	Lifetime
NA	diverse αβ integrins	<0.25 μm	small dot-like	leading edge	Talin, paxillin	Short-lived (2-3 min)
FX	diverse αβ integrins	<1 μm	dot-like	cell periphery	Talin, vinculin, FAK, paxillin	Short-lived, (2-3 min)
FA	diverse αβ integrins	~0.25 – 5 μm	long	centrally located	Talin, vinculin, FAK, paxillin, α-actinin, zyxin	long-lived (mostly <10 min, some ~100 min)
FB	α5β1 & diverse αβ Integrins	~5–10 μm	streaks	Centrally located	Talin, vinculin, FAK, paxillin, α-actinin, zyxin, tensin	long-lived >1 h
Invadosome	various αβ integrins but excludes αVβ5	<5 μm	punctate	ECM interaction sites	Talin, vinculin, FAK, paxillin, α-actinin, zyxin, tensin, Arp2/3, (N-)WASP	long-lived >1 h
RA	αVβ5	-	ring-like	Static sites	Clathrin, numb, dab2	long-lived >7 h

Note: This is a partial list of associated proteins. For further details, please refer to the following sources:(Linder 2009; Bachir *et al.* 2014; Zuidema *et al.* 2018, 2020; Lock *et al.* 2019; Baschieri *et al.* 2020; Nolte *et al.* 2021; Chastney *et al.* 2021; Mishra and Manavathi 2021; Alfonzo-Méndez *et al.* 2022; Yamaguchi and Knaut 2022).

Distinct regions of a migrating cell encounter varying levels of mechanical force. Mechanical force is an important deciding factor of the type of adhesion complex. Greater force leads to more mature and stable types of adhesion complexes. This results in region-specific adhesion complex localization (Parsons *et al.* 2010).

Filopodia are slender, actin-rich protrusions from a cell's leading edge, exploring the extracellular matrix (ECM) and guiding cellular movement. They adhere to the ECM through transient integrin-based complexes. These

complexes, less stable due to minimal force, quickly disassemble but include proteins like myosin-X for actin regulation and mechanosensitivity. Behind the filopodia lies the lamellipodia, where nascent adhesions (NAs) form under slightly higher mechanical stress (He *et al.* 2017), leading to more stable focal complexes (FXs). FXs, which may evolve from NAs, are small yet crucial in the hierarchical assembly of proteins that link the actin cytoskeleton to the ECM via intracellular connectors like talin (Chastney *et al.* 2021). When conditions are right, FXs can mature into larger, more robust focal adhesions (FAs), recruiting additional elements such as zyxin and alpha-actinin to strengthen the integrin-actin connection (Bachir *et al.* 2014). High mechanical forces transform FAs into fibrillar adhesions (FBs), marked by tensin and α5β1 integrin, with tensin replacing talin as the main actin linker. FBs, anchoring to actin stress fibers' ends, stretch fibronectin in the ECM, unveil new binding sites, and foster fibrillogenesis. These fibrils scaffold ECM protein deposition, allowing cells to remodel the ECM (Cukierman *et al.* 2001).

Cells also feature specialized structures like podosomes and invadopodia, which degrade the ECM to aid invasion. Podosomes are common in macrophages and osteoclasts, while invadopodia are typical in cancer cells. These structures contain cortactin, neural Wiskott-Aldrich syndrome protein (N-WASP), and the actin-related protein 2/3 (Arp2/3) complex, promoting actin polymerization and recruiting matrix metalloproteinases for ECM breakdown (Linder 2007).

Integrins trigger various signaling pathways by attracting proteins like Focal Adhesion Kinase (FAK), Src kinases, and phosphoinositide 3-kinases (PI3K). These proteins activate downstream effectors, including extracellular signal-regulated kinases (ERK), protein kinase b (Akt), c-jun N-terminal kinases (JNK), and the rho family of GTPases. Rho-induced myosin contractility moves actin filaments, engaging talin and fortifying adhesions (Zaidel-Bar *et al.* 2004). Inter-pathway communication fine-tunes these interactions, orchestrating diverse cellular outcomes such as survival, growth, differentiation, structural reorganization, movement, adhesion, and polarity (Legate *et al.* 2009).

The adhesome is a collective term for the many adaptor proteins that connect integrins to the cytoskeleton, as well as the various enzymes and signaling proteins that control the dynamics of adhesion sites (Zaidel-Bar *et al.* 2007; Bachir *et al.* 2014). The integrin adhesome comprises several thousand proteins (Geiger and Zaidel-Bar 2012). A consensus adhesome refers to a core set of proteins that are commonly found across various adhesion complexes. There are around 60 core proteins identified to belong to consensus adhesome through experiments, proteomic analysis, and literature search (Kanchanawong and Calderwood 2023).

1.3 Reticular adhesion

Reticular adhesions (RAs) are a newly identified type of integrin-based cell-ECM adhesion complexes, characterized by the presence of αVβ5 integrin and flat clathrin lattices (FCLs). Unlike other adhesion complexes that disassemble before cell division, RAs allow cells to stay anchored to the ECM during significant cytoskeletal changes (Grove *et al.* 2014; Lock *et al.* 2018).

While αVβ5 integrin typically binds to ECM proteins like vitronectin to form focal and fibrillar adhesions (Burridge *et al.* 1988; Cheresh *et al.* 1989), fibronectin inhibits RA formation by activating integrin α5β1 at fibrillar adhesion sites. This activation prevents the assembly of both RAs and FCLs (Hakanpää *et al.* 2023). RAs are thought to arise from frustrated endocytosis, especially under low mechanical force, when cells cannot fully internalize ECM components, leading to the persistence of FCLs. RAs help cells adhere to their environment without the need for cytoskeletal support, particularly useful during cell rounding before division (Lukas *et al.* 2024).

Cell-ECM adhesion regulates the cell cycle, with increased adhesion areas corresponding to contractile force generated during the G1 to S phase transition. This force is produced by CDK1-cyclin complexes phosphorylating Filamin A, leading to actin polymerization and stress fiber formation. As cells progress to the G2 phase, these complexes deactivate, reducing force and adhesion areas (Cukier *et al.* 2007; Fededa and Gerlich 2012; Jones *et al.* 2018). During early mitosis, β1 integrins recede from ECM proximity, allowing cells to round up by detaching from the ECM and reorganizing their cytoskeleton (Harris 1973; Kamranvar *et al.* 2022). Contrary to previous beliefs, cells maintain some adhesion during mitosis through αVβ5 integrins, forming RAs that are crucial for orienting the mitotic axis (Théry *et al.* 2005; Lock *et al.* 2018). Disruption of RAs can lead to abnormal division and affect spindle orientation, which is vital for proper chromosome distribution to daughter cells (Högnäs *et al.* 2012; Lancaster *et al.* 2013). The positioning of RAs acts as a spatial memory, ensuring the spindle aligns with the cell's pre-rounding orientation, thus influencing the plane of cell division (Théry *et al.* 2005, 2007; Yennek *et al.* 2014; Lock *et al.* 2018).

1.3.1 Clathrin-mediated endocytosis and RA

Clathrin-mediated endocytosis (CME) is a process where cells internalize molecules and particles from their surroundings using clathrin-coated vesicles. Clathrin forms a trimeric complex, each unit consisting of a heavy chain weighing approximately 191 kDa. These heavy chains are bound to light chains, each ranging between 23-27 kDa in mass. This configuration is reminiscent of a three-legged design, which is also known as a triskelion structure. This structure interlocks to produce the characteristic clathrin lattice (Pearse 1976; Wood and Smith 2021). FCLs have been found to colocalize with RAs (Lock *et al.* 2018). They are flat sheets of clathrin hexagons found on the cytoplasmic surface of the plasma membrane (Heuser and Evans 1980). FCLs are much larger and more

stable than another commonly found clathrin-made membrane structure called clathrin-coated pits (CCPs), which are involved in endocytosis (Grove et al., 2014). Clathrin adaptor proteins (APs) are well-studied for their roles in the formation of clathrin coats and the sorting process at the Golgi apparatus and plasma membrane (Schmid 1997). They are composed of four subunits and exist in various forms. Among them, AP-1 and AP-2 are the most common. During the CME, adaptor proteins bind to the membrane, select and tag receptors for internalization as cargo, and recruit clathrin. The AP-2 complex, a central adaptor protein in CME, consists of two large subunits (α and β), a medium subunit (μ) for identifying cargo, and a small subunit (σ) that aids in the complex's stability and assembly. It binds to the cytoplasmic membrane by interaction with phosphoinositide headgroups of Phosphatidylinositol 4,5-bisphosphate (PI(4,5)P2). It selects the cargo by recognizing specific amino acid sequences on receptor cytoplasmic tails. After catching the receptors, the AP-2 complexes come together and cluster. By clustering with other active AP-2 complexes, binds to clathrin through β-active sites. In these triple interactions, the AP-2 complex plays a pivotal role in forming the clathrin lattice and other endocytosis structures (Boucrot *et al.* 2010; Kaksonen and Roux 2018).

The formation of RAs is thought to be driven by several distinct mechanisms. The first is frustrated endocytosis, which involves the CME machinery and prevents integrin αvβ5 from being internalized by the cell, leading to its accumulation and the subsequent formation of RAs. Additionally, FCL formation has been identified as a requirement for the clustering and stability of αvβ5. Notably, integrin αvβ5 is also essential for the formation of FCLs. Furthermore, evidence suggests the co-assembly of FCLs and integrin αvβ5 clusters (Zuidema *et al.* 2022; Hakanpää *et al.* 2023).

1.3.2 Cell migration and RA

Cell migration is an important process for organismal development, wound healing, and the progression of diseases, made possible by a combination of mechanical forces, biochemical signals, and environmental factors. In the classical model of mesenchymal migration, cells move by projecting a lamellipodium, securing to a substrate, and pulling themselves forward, a mechanism especially observed on flat, two-dimensional planes (Abercrombie 1980). However, this migration is not a sequence of isolated events but rather a concurrent series of actions (De Pascalis and Etienne-Manneville 2017). Migration occurs as cells extend forward and simultaneously retract at the rear, with integrins playing an essential role in stabilizing these movements by anchoring the cytoskeleton to the extracellular matrix. Integrins are vital for the migration of individual cells, as they detect and respond to external cues and mechanical forces (Sheetz *et al.* 1998). This function is facilitated by the conformational changes in integrins when they bind to the extracellular matrix or internal proteins, affecting their binding strength, aggregation, and the attraction of cytoskeletal connecting proteins (Hynes 2002). These interactions enable cells to apply and react to mechanical forces, forming new adhesions at the leading edge

and breaking them down at the trailing edge. Protrusive forces arise from actin polymerization, which does not rely on myosin, while contractile forces are generated by myosin II, which attaches to actin and utilizes ATP for movement (De Pascalis and Etienne-Manneville 2017; Oakes *et al.* 2018).

Optimal cell migration is dependent on clathrin-mediated endocytosis (CME), as evidenced by the cell migration defects observed when clathrin or its adaptors are inhibited (Maritzen *et al.* 2015). CME involves creating clathrin-coated structures (CCSs) inside the plasma membrane, comprising clathrin and adaptors for receptor recruitment (McMahon and Boucrot 2011). CCSs join disassembling focal adhesions to internalize integrins, aiding adhesion disassembly and cell movement(Ezratty *et al.* 2009). The balance between the formation of focal adhesion and their disassembly regulates both haptotaxis, the guided movement of cells along ECM gradients, and durotaxis, the migration towards varying substrate stiffness (Nishimura and Kaibuchi 2007). The stiffness of the ECM determines the magnitude of mechanical force experienced by a cell. High mechanical forces on ECM-bound β3-integrin result in adhesion, while lower forces lead to CME via interaction with the adaptor Dab2 (Yu *et al.* 2015). There is an optimal stiffness level of the ECM that enhances cell migration.

Clathrin-coated structures (CCSs) such as FCLs contribute to cell migration beyond their role in endocytosis (Grove *et al.* 2014). These FCLs function as signaling hubs for various receptor tyrosine kinases and are recognized as adhesion structures (Grove *et al.* 2014; Baschieri *et al.* 2018). They provide a scaffold for the assembly of receptors and regulatory proteins. A pivotal element in FCL formation, αVβ5 integrin, shuttles between focal adhesions and FCLs (Zuidema *et al.* 2018; Baschieri *et al.* 2018). These FCL-based adhesion structures, dependent on αVβ5 integrin clustering, are now known as reticular adhesions (Lock *et al.* 2018, 2019; Baschieri *et al.* 2018). In a stationary state, FCLs and RAs offer stable anchorage to the ECM. However, for a cell to migrate, it must disengage these adhesion complexes (Saffarian *et al.* 2009; Elkhatib *et al.* 2021; Hakanpää *et al.* 2023).

Integrin α5β1 binds to ECM molecule fibronectin (FN). This attachment forms focal and fibrillar adhesion. Fibronectin's activation of integrin α5β1 is a critical factor in cell migration (Pankov *et al.* 2000). Integrin α5β1 plays a dual role in tumor progression, acting as a promoter or inhibitor of cancer depending on the cell type and origin (Akiyama *et al.* 1995). The 2023 study by Hakanpää et al. focused on how FN affects the formation of RAs. Their research showed that an ECM enriched with FN is associated with fewer FCLs and RAs, suggesting FN's potential role in their suppression. The study further revealed that FN's inhibitory action is mediated through the activation of integrin α5β1 at tensin1-positive fibrillar adhesions, which is crucial in preventing RA formation. Additionally, the absence of RAs following the inhibition of the CME machinery underscores the importance of a functional CME system for RA development. The study also proposed that the transformation of static RAs into more dynamic focal adhesions (FAs) is essential for cell migration (Hakanpää *et al.* 2023).

1.4 History of cell-ECM adhesions and reticular adhesion research

Since the realization of the ECM's influence on cellular behavior and organogenesis (Grobstein and Parker 1954), the study of cell-ECM interaction has been a very active area of research to this day (Chastney *et al.* 2021). In 1906, Harrison disproved the idea that tissues were merely one continuous mass, showing instead that they were made up of separate cells (Harrison 1906). This led to a new question: How do these individual cells stick together within the tissues (Lewis 1922)? This question initiated a research effort to understand cellular connections. The chemo affinity hypothesis was an early attempt to answer this, suggesting that cell-cell connection is a chemical interaction (Sperry 1963). In the 1950s and 1960s, the use of fibroblast cells in *in vitro* studies, along with the exploration of viral transformation, significantly propelled the field of cell-cell adhesion research forward (Abercrombie and Heaysman 1953; Stoker and Rubin 1967; Stoker *et al.* 1968). At the same time, researchers began to uncover the profound influence of the ECM on cellular behavior, tissue differentiation, and organogenesis, marking the genesis of cell-ECM adhesion research. The advent of interference reflection microscopy and electron microscopy in cell biology research provided direct visualization of adhesion sites, accelerating our understanding of cellular interactions. This enabled the observation that adhesions are specific, localized contacts on culture substrates (Curtis 1964; Izzard and Lochner 1976; Heath and Dunn 1978). The focus then shifted towards identifying specific adhesion molecules responsible for cell-ECM interactions (Thiery *et al.* 1977; Takeichi 1977; Müller and Gerisch 1978; Rutishauser *et al.* 1978; Bertolotti *et al.* 1980; Yoshida and Takeichi 1982). Proteins such as actin were isolated using sodium dodecyl sulfate-polyacrylamide gel electrophoresis, and specific fluorescently labeled antibodies were employed to map their locations at adhesion sites (Lazarides and Weber 1974). Similarly, α-actinin antibodies were shown to line up along actin filaments and other components (Lazarides and Burridge 1975). This method also led to the discovery of vinculin and talin, two new proteins that specifically localize to adhesion sites (Geiger 1979; Burridge and Connell 1983). Fibronectin was found in the adhesion sites and aligned with actin filaments, indicating cells attach to a particular matrix protein, not just the culture surface (Hynes and Destree 1978). Identifying integrins as cell-ECM adhesion receptors was a significant achievement in this research effort (Tamkun *et al.* 1986). Integrins were soon realized as central figures in the study of cell-ECM adhesion (Hynes 1987).

In 1971, the first evidence linked clathrin plaques to cell-ECM adhesion (Abercrombie *et al.* 1971). By 1999, it was understood that the fate of nascent focal adhesions, whether they disassemble or mature, hinged on Rho-regulated myosin contractility (Flinn and Ridley 1996; Garcia *et al.* 1999). The early 2000s saw questions arise about the role of clathrin in the disassembly of focal adhesions, with 2001 highlighting the targeting of mature focal adhesions by clathrin for disassembly(Zamir *et al.* 1999; Laukaitis *et al.* 2001). The mid-2000s brought significant insights, marking the discovery that clathrin adaptors like

Dab2 and ARH are involved in focal adhesion disassembly. This period also saw the identification of flat clathrin lattices (FCLs) as adhesive structures (Akisaka *et al.* 2008; Ezratty *et al.* 2009). By 2010, advances in imaging techniques had significantly enhanced our understanding of the molecular composition and dynamics of adhesion complexes (Ezratty *et al.* 2009; Worth and Parsons 2010). By now it was clear that Cell-ECM adhesion is vital for tissue structure and function. Its disruption was linked to diseases such as arthritis, cancer, osteoporosis, and atherosclerosis (Parsons *et al.* 2010). For instance, in cancer, the adhesion of cancer cells is often reduced compared to normal cells (Shin *et al.* 2017). Researchers started targeting the cell-ECM adhesion process to develop potential therapeutic strategies to treat or prevent the progression of these diseases (Mousa 2008). The following years, particularly 2012 and 2014, were pivotal in understanding the maturation of nascent adhesions and the colocalization of FCLs with plasma membrane receptors (Wehrle-Haller 2012; Grove *et al.* 2014). By 2016, the focus shifted to the specific adaptors involved in recruiting integrins to adhesive clathrin plaques, with AP2 emerging as a key player (Lampe *et al.* 2016). The subsequent years, up to 2019, saw FCLs recognized as signaling platforms and cell-ECM adhesions (Leyton-Puig *et al.* 2017; Lock *et al.* 2018, 2019). Recent research from 2022 to 2023 has further elucidated the role of integrin αVβ5 in FCLs and RAs, cementing the importance of these structures in cellular adhesion and signaling (Alfonzo-Méndez *et al.* 2022; Kanchanawong and Calderwood 2023; Hakanpää *et al.* 2023).

1.5 Reconstitution experiments

To fully grasp the intricacies of cellular processes, experiments on living cells alone are insufficient. Complementing this, reconstitution studies adopt a reductionist approach, which involves breaking down complex systems into simpler, fundamental elements. Understanding cellular processes requires more than just live-cell experiments. Reconstitution studies using cell-free extracts or purified proteins have deepened our knowledge of cell biology (Bock *et al.* 1998; Liu and Fletcher 2009). Eduard Buchner's discovery of cell-free fermentation in 1897 laid the groundwork for these experiments, challenging the notion that life processes could only occur within living cells. This paved the way for significant advancements, such as Albert Szent-Györgyi's reconstitution of muscle contraction systems (Szent-Györgyi 1942) and Arthur Kornberg's synthesis of DNA *in vitro* (Lehman *et al.* 1958). Over time, reconstitution studies have evolved from analyzing simple molecules to recreating entire functional units, allowing for the replication of complex cellular functions like the cytoskeleton and signaling pathways (Barlowe 1994; Nurse 2007). These experiments now integrate systems biology data to better mimic physiological conditions, leading to a more profound understanding and accurate modeling of cellular mechanics.

Solid-supported lipid bilayers or membrane sheets are invaluable for simulating the cell's surface, enabling the study of cellular behaviors and interactions. These bilayers are accessible to various surface-specific analytical methods, facilitating detailed research into cell adhesion, signaling, ligand-

receptor dynamics, enzymatic surface reactions, and pathogen attacks. Cell unroofing is a technique that unveils the cytoplasmic side of the cell membrane by creating membrane sheets from live cells (Heuser 2000). This method is crucial for understanding cellular interactions and is influenced by the stiffness of the substrate, which affects cell adhesion properties. The advent of cell unroofing in the 1970s marked a significant advancement in the ability to image cellular membranes, overcoming challenges posed by their fluidity. This process involves mechanically isolating the membrane using techniques that have become essential in conjunction with electron microscopy for visualizing cellular structures (Nermut 1982). For observation, cells are first anchored to a substrate with adhesion agents like poly-L-lysine. The controlled disruption follows, separating the membrane for isolated examination, crucial for analyzing membrane structure and function without cytosolic interference. There are many methods used for the unroofing of cells. Ultrasonication and squashing-peeling are two popular unroofing methods. In the ultrasonication method of unroofing, high-frequency sound waves create bubbles within the cytosol. When these bubbles collapse, they release energy as shockwaves. These shockwaves cause bursting of the plasma membrane, typically the apical side, and the release of cytosol. When the debris is washed away it leaves the basal membrane as membrane sheets on a solid substrate. On the other hand, the squashing-peeling method attaches two solid substrates to both sides of the cells and squashes the cells to induce rupture. Then the ruptured cells are peeled apart. This leaves the apical membrane attached to one substrate and the basal membrane attached to another (Heuser 2000). Cell unroofing is vital for studying integral membrane proteins, providing direct access to their intracellular domains for high-resolution structural analysis.

Membrane sheets are excellent for *in vitro* assays, aiding in the exploration of actin polymerization, exocytosis, and endocytosis, essential for understanding cell motility, structure, and communication. In Total Internal Reflection Fluorescence (TIRF) microscopy, cell unroofing provides signal clarity, removing internal fluorescent molecules to focus on membrane-associated proteins. The technique's evanescent wave illuminates a thin section near the coverslip, allowing high-contrast imaging of membrane events, free from non-membrane-bound protein interference, thus enhancing TIRF microscopy's specificity in visualizing membrane-associated proteins (Fish 2009). The study of focal adhesions (FAs) and integrin-mediated extracellular matrix (ECM) adhesion has traditionally been conducted on two-dimensional substrates. These investigations have provided insights into cell anchoring and migration (Reinhard *et al.* 1995; Chrzanowska-Wodnicka and Burridge 1996).

In vitro systems are instrumental in manipulating adhesion components to study the effects on the structure and function of cell-ECM adhesions. They enable the identification of essential core components and additional non-

canonical elements that may provide specialized functions. Through *in vitro* reconstitution, the spatial and molecular architecture of an adhesion complex can be analyzed, shedding light on their role in mechanotransduction and response to receptor trafficking. The *in vitro* environment also allows for real-time observation of adhesion complex dynamics, including their formation, maturation, and disassembly, offering insights into their lifecycle and adaptability. Furthermore, it facilitates the exploration of the regulatory mechanisms of adhesion complexes, observing their reaction to cellular signals and disturbances. This research is crucial for understanding their role in health and disease, potentially guiding the development of therapeutic interventions.

1.6 Research questions and hypotheses

The mechanisms behind the dynamic formation of RAs and their physiological triggers remain elusive. The interdependent formation of FCLs and RAs requires more investigation. An approach to addressing these questions involves the *in vitro* reconstitution of RAs, facilitating a detailed examination of the assembly process.

The aim of this study is to prepare membrane sheets and reconstitute reticular adhesions on them.

The study's objectives included optimizing cell unroofing techniques to produce membrane sheets and analyzing them with TIRF microscopy. It aimed to reconstitute RAs. The research also sought to understand how factors like time and temperature affect their formation.

2 MATERIALS AND METHODS

2.1 Buffers and antibodies

In the course of this study, two specialized buffer solutions were employed. The ultrasonication buffer, which was utilized to fill the dish containing the cells during the process of ultrasonication unroofing, consisted of 15 mM 4-(2-hydroxyethyl)-1-piperazineethanesulfonic acid (HEPES) at a pH of 7.3, 15 mM potassium chloride (KCl), 1 mM ethylene glycol-bis(β-aminoethyl ether)-N, N, N′, N′-tetraacetic acid (EGTA), and 1 mM magnesium chloride ($MgCl_2$). The cytosolic buffer, employed for the dilution of the cytosol as well as for the washing and maintenance of the live membrane sheets before fixation, included 15 mM HEPES (pH 7.3), 70 mM KCl, 1 mM EGTA, and 1 mM $MgCl_2$. The composition of the buffer solutions was refined based on formulations previously utilized for analogous experimental purposes (Peeler *et al.* 1993a; Reilein and Nelson 2005).

For the immunofluorescence staining, antibodies targeting Tensin-1, talin-1, vinculin, paxillin, focal adhesion kinase (FAK), phosphorylated-FAK (p-FAK), and numb were utilized. Details regarding the primary and secondary antibodies—including their host origin, clonality, fluorescent conjugates, and providers—are documented in Appendix 1.

2.2 Cell line generation

Two cell lines were used in this study which were generated during a previous study (Hakanpää *et al.* 2023). These cell lines were: U2Os-ITGB5-mScarlet and U2Os-AP2-Halo. The process involved designing guide RNA (gRNA) sequences, which were obtained from Integrated DNA Technologies. This design was made easier by using the Wellcome Sanger Institute Genome online editing tool (https://wge.stemcell.sanger.ac.uk//). Afterward, the gRNAs were inserted into the pSpCas9(BB)-2A-Puro (PX459) V2.0 vector, kindly provided by Dr. Feng Zhang (Addgene plasmid #62988), using BbsI restriction sites. This cloning was verified through Sanger sequencing. To achieve homologous recombination, the gRNAs were transfected together with the donor template. The gRNA sequence for the U2Os-ITGB5-mScarlet line was 5′−CAAATCCTACAATGGCACTG−3′, and for the U2Os-AP2-Halo line, it was 5′−TGCTACAGTCCCTGGAGTGA−3′. The complete sequences for the donor templates are provided in Appendix 2. The U2Os-ITGB5-mScarlet line was employed as the donor of membrane sheets, featuring integrin beta 5 conjugated to the fluorescent marker mScarlet. Conversely, the U2Os-AP2-Halo line was utilized as the source of cytosolic components, marked by the presence of Halo-tagged adaptor protein complex 2 sigma subunit (AP-2-σ).

2.3 Cell culture and maintenance

Cells were grown on MatTek culture dishes (MatTek corporation, Ashland, MA). They are a type of petri dish tailored for growing cells and conducting microscopic examinations. These dishes merge the practicality of regular disposable plastic petri dishes with the clarity of glass bottoms, ensuring that microscopic images of cells are highly detailed. The culture medium employed was Minimum Essential Medium (MEM), which was enriched with a 10% v/v fetal bovine serum (FBS), and a 100 units/mL penicillin-streptomycin solution both procured from Thermo Fisher Scientific, Vantaa, Finland. The cells were incubated under optimal conditions, maintaining a temperature of 37°C and an atmosphere containing 5% CO_2. To ensure continued growth and viability, the cells underwent regular passaging at intervals determined by their confluency and growth kinetics.

2.4 Coating of imaging dishes

Before cell seeding, MatTek culture dishes and square coverslips (24 x 24 mm^2) were coated with a 0.01% (0.1 mg/ml) poly-L-lysine (PLL) solution (MP Biomedicals, Illkirch Graffenstaden, France) and incubated at 37°C for at least one hour to ensure adequate adsorption of PLL. Then the PLL solution was aspirated from each well, and the coverslips were rinsed thrice with 1 mL of phosphate buffer saline (PBS) to remove any unbound PLL.

2.5 Cell unroofing

Two methods were tested for the preparation of the membrane sheets: the ultrasonication method and the squashing-peeling method. Cells for ultrasonication were grown on MatTek dishes, while those for squashing-peeling were on 24 x 24 mm^2 cover slips residing in 6-well plates. After the PLL coating, cells were seeded with fresh media at densities of approximately 76,000 cells and 480,000 cells for a Mattek dish and each well of 6-well plates respectively. The culture vessels were then placed in a humidified incubator at 37°C with 5% CO_2 and left for two days or until the cells attained the desired 100% confluency, with medium changes performed as required.

2.5.1 Ultrasonication based cell unroofing

Ultrasonication of the cells was performed using a homogenizer (SONOPULS HD 2070, BANDELIN electronic GmbH & Co. KG, Berlin, Germany) with a titanium microtip (MS73, BANDELIN electronic GmbH & Co. KG, Berlin, Germany). Following the attainment of 100% confluency, the standard culture medium was gently removed, and the MatTek dishes were subsequently filled to capacity with the ultrasonication buffer. The hypotonic nature of this buffer was specifically chosen to facilitate the process of cell unroofing.

Upon the swift replacement of the culture medium with the ultrasonication buffer, the titanium microtip was immersed in the buffer solution. Ultrasonication was promptly initiated to minimize any potential alterations to the cellular environment. The microtip's position was precisely controlled, maintaining a consistent height of 8 mm above the base of the Mattek dish. This strategic placement is of paramount importance as it directly affects the distribution of ultrasonic energy and the shear forces generated, which are critical factors in achieving optimal cell unroofing while preserving the integrity of the cellular components.

The ultrasonication process was meticulously controlled and varied across a range of parameters to assess their impact on cell lysis efficiency. The temperature conditions were set at two distinct points: a low-temperature setting of 4 °C to minimize enzymatic activity and prevent degradation of cellular components, and a physiological temperature of 37 °C to simulate conditions within a living organism. The power output of the homogenizer was adjusted to two levels, 10 W and 20 W, to evaluate the effect of ultrasonic intensity on cell disruption. Additionally, the number of pulses was modulated, with a range from 1 to 4 pulses, to determine the optimal pulse number for effective cell lysis without excessive damage to the cellular material.

2.5.2 Squashing-peeling based cell unroofing

After growing the cell confluently on PLL-coated square coverslips (24 x 24 mm^2), the culture medium was replaced with this cytosolic buffer. The formation of the membrane sheet was induced by applying gentle pressure to the round coverslip using a Champagne bottle stopper cork. This pressure was maintained momentarily before the cork was swiftly removed. The resultant membrane sheet was then immediately washed with ice-cold cytosolic buffer to remove any non-adherent cellular components. The freshly prepared membrane sheet was maintained in ice-cold cytosolic buffer to preserve its integrity. The subsequent assay procedures must be conducted within a 20-minute window following the preparation to ensure optimal results.

2.6 Membrane staining

The fixed membrane sheets were stained with a 5 µg/mL solution of Wheat Germ Agglutinin Fluorescence dye conjugate, CF405S WGA (Biotium, Inc., Fremont, CA, United States). When the live cells were stained with CF405S WGA, the solution was prepared by mixing with culture media. the plate was gently swirled to distribute the stain evenly. The plate was incubated at 37°C or on ice for 25 minutes; the higher temperature allowed staining of the plasma membrane and internal organelle membranes, while the colder condition restricted staining to the cell surface. Following incubation, the WGA solution was removed, and the coverslips were rinsed thrice with 1 mL of PBS before discarding the PBS.

Alternatively, the membrane sheets were also stained with Caax-CFP plasmid containing a cyan fluorescent protein (CFP) fused to a membrane-targeting sequence (Caax). The transfection of cells with Caax-CFP was performed in a 12-well plate, where cells were cultured to achieve 70-80% confluency, ensuring optimal density for transfection efficiency. The process began with the preparation of a transfection mixture consisting of 4 µL of Polyethylenimine (PEI) reagent (with a concentration of 225 ng/µL) and 300 ng of plasmid DNA, combined in 200 µL of opti-MEM media (Thermo Fisher Scientific, Waltham, MA, United States) This mixture was vortexed for 10 seconds to achieve a homogenous solution, adhering to a 3:1 PEI to DNA ratio, which is critical for forming stable PEI-DNA complexes. The PEI-DNA mixture was then incubated at room temperature for 15-20 minutes, during which the cell culture media in the wells were replaced with 500 µL of warm fresh media to prepare the cells for transfection. Following the incubation period, the PEI-DNA complexes were added dropwise to the designated well, and the plate was gently agitated to ensure even distribution of the complexes across the cell monolayer. To further enhance transfection efficiency, the plate underwent centrifugation at 1200 rpm for 5 minutes, a step that promotes closer contact between the PEI-DNA complexes and the cell surface, thereby facilitating cellular uptake. Subsequently, the plate was transferred to an incubator set at 37°C with 5% CO_2 for a duration of 4 hours, allowing the cells to internalize the PEI-DNA complexes. An optional step following this incubation involves replacing the transfection media with fresh complete media to provide the cells with nutrients necessary for recovery and expression. The cells were then incubated for an additional 24-48 hours to permit gene expression and protein synthesis.

The unroofed cells were also stained with 4',6-diamidino-2-phenylindole (DAPI) for detection of DNA.

2.7 Preparation of cytosol

U2Os-AP2-Halo cells were extensively propagated across twelve 20 cm dishes. To ensure the removal of all traces of media, the culture was gently washed with phosphate-buffered saline (PBS). Utilizing a cell scraper, the adherent cells were carefully detached from the surface of the culture dish. The resultant cell suspension was then collected into a conical centrifuge tube for subsequent processing. Then cells underwent centrifugation at 1200 rpm for 3 minutes. The supernatant was discarded, and the cell pellet was resuspended in 1 mL of ice-cold cytosolic buffer, supplemented with an anti-protease tablet, and maintained on ice. Cell lysates were then subjected to three rounds of sonication, each consisting of five 30-second cycles interspersed with 30-second intervals of rest, utilizing Bioruptor water bath sonicator (Diagenode, Seraing, Belgium).

Rat brains, obtained from the Jette Lengefeld laboratory, were homogenized in cold cytosolic buffer (1 mL per brain) with Heidolph homogenizer (Heidolph, Schwabach, Germany) at 1500 rpm with 10-15 strokes.

After the addition of anti-protease, the homogenate was centrifuged at 10000xg for 20 minutes, and the resultant supernatant was collected.

The measurement of protein concentrations in cellular and brain extracts was performed using the Denovix Quantification Spectrophotometer (DeNovix Inc., Wilmington, DE, USA) and the Bicinchoninic Acid (BCA) assay kit (Thermo Fisher Scientific, Waltham, MA, USA). A calibration curve was created with bovine serum albumin (BSA) standards to assist in the calculation of protein concentrations in unknown samples, which were appropriately diluted. The method involved assigning standards, samples, and a blank to designated wells or tubes, followed by the addition of a working solution made from BCA reagents. After incubation, the optical density was measured at 562 nm, facilitating the calculation of protein concentrations by comparing the absorbance of the samples with the calibration curve.

In a subsequent step, U2Os-AP2-Halo cytosolic extract was mixed with rat brain extract in a 1:2 ratio to increase the protein concentration. A cytosolic buffer was formulated to obtain a final protein concentration of 5 mg/mL, which was utilized in the following reconstitution experiments.

2.8 Reticular adhesion reconstitution

At first, the membrane sheet was incubated solely in a buffer solution, devoid of cytosolic components, to serve as a baseline control for the reconstitution analysis. It was also incubated with AP2 halo sigma ligand fluorophore. This membrane was also stained immunofluorescently for numb. This step was critical to exclude the pre-existence of adhesion complexes and clathrin-mediated endocytosis (CME) structures. Different temperatures and incubation times were tested for their effects on the result. The temperature were 4 and 37°C and the incubation time was 5, 10, and 20 minutes. During incubation, the JFX 646 Halo tag was introduced into the cytosol to achieve a diluted concentration of 1 μM. 2 mM Mg-ATP, adenosine triphosphate bound to a magnesium ion, was also added. When the incubation was over, the cytosol was removed, and the membrane sheet was washed with ice-cold cytosolic buffer.

2.9 Visualization of AP-2 Halo

The Janelia Fluor HaloTag Ligand 646 (Promega Corporation, New York, USA) was utilized for visualizing the HaloTag fusion AP-2-σ proteins within the cytosol. A 200μM stock solution was prepared using DMSO. This stock was utilized at a 1:1000 dilution using the cytosol to stain live membrane sheets, concurrently with cytosol incubation. The membrane sheets were incubated for 5 minutes, following which they were washed with an ice-cold cytosolic buffer. After the staining process, the membrane sheets were fixed to preserve the fluorescent labeling.

2.10 Fixation

Fixation of the membrane sheets after reconstitution of reticular adhesion was done without any delay by incubating the membrane sheets with 4% paraformaldehyde (PFA) solution at room temperature for 20 min. Membranes were washed thrice with PBS and kept in ice-cold PBS.

2.11 Immunofluorescence staining

The membranes were blocked using 1% BSA for a minimum of five minutes at ambient temperature. The primary antibody is then diluted in 1% BSA at a 1:300 ratio. The primary antibody solution is dispensed onto fixed membrane sheets and incubated for 30 minutes at room temperature in the dark. Following a triple wash with PBS, the secondary antibody conjugated to a suitable fluorophore is similarly diluted in 1% BSA, applied to the membranes, and incubated in darkness for 30 minutes before a final wash with PBS. The primary antibody and secondary antibody used are listed in Appendix 5. A final 5-minute fixation step with 4% PFA was done.

2.12 Microscopy

TIRF microscopy of fluorescently stained fixed membrane sheets was performed using an ONI Nanoimager microscope (Oni Ltd, Banbury Road, Oxford, United Kingdom) with an oil immersion 1.49 NA 100 × super achromatic objective (Olympus Corporation, Japan). The setup included four built-in lasers with wavelengths of 405 nm, 488 nm, 561 nm, and 640 nm, with power and exposure times tailored to the experiment's needs. The excitation angle was set between 30° and 55° to induce total internal reflection. Images were captured by the Nanoimager's ORCA-Flash4.0 V3 digital complementary metal-oxide-semiconductor (CMOS) camera (Hamamatsu Photonics, Japan) with field of view of 50µm x 80µm and exposure times of 500 or 1,000 or 1,500 ms. The image acquisition software used was NimOS. Image captures were performed at room temperature, ensuring consistent environmental conditions throughout the experiment.

2.13 Image analysis

Using Fiji ImageJ V1.53t, the acquired images underwent processing and analysis with a custom macro to automate the counting and sizing of reticular adhesions (RAs). The macro employed color thresholding and hue, saturation and brightness (HSB) stack conversion to isolate and highlight the RAs, followed by binary masking and image calculation to create a composite image. Particle analysis was then applied to this image, quantifying the RAs with precise scale settings for accurate size representation. The results, including RA counts and sizes, were tabulated and overlaid on the images for visual confirmation. Detailed macro code is provided in the appendix for reproducibility and reference.

2.14 Statistics

Microsoft Office 16 Excel was utilized for the statistical computations. The mean unroofing yield for each method was calculated using the AVERAGE function in Excel. In the comparative analysis, the sample standard deviation (sd) was computed for each unroofing method's yield utilizing the STDEV.S function within Microsoft Excel. Subsequently, the standard error of the mean (SEM) was ascertained by dividing the sample standard deviation by the square root of the sample size n. To visually convey the variability inherent in each method, error bars corresponding to the SEM were integrated into the bar graph. These error bars were customized in Excel to accurately reflect the SEM values calculated for both the ultrasonication and squashing-peeling unroofing yield. Furthermore, an independent samples t-test was executed to evaluate the statistical discrepancy between the ultrasonication and squashing-peeling unroofing yield.

3 RESULTS

3.1 Isolation of membrane sheets

In this study, two methodologies were evaluated for cellular unroofing: ultrasonication and squashing-peeling. The unroofing process aimed to remove the apical membrane along with all cytoplasmic components, ensuring that only the basal membrane remained intact upon the solid substrate. To enhance the visibility of the membrane sheets after unroofing, they were stained with a wheat germ agglutinin (WGA) conjugated with a fluorophore. This conjugate selectively binds to the membrane-associated saccharides N-acetylglucosamine and sialic acid. Additionally, the fixed membranes were incubated with 4′,6-diamidino-2-phenylindole (DAPI), a fluorescent stain that targets AT-rich regions within DNA, to ascertain the presence of any residual cell nuclei. The existence of nuclei served as a marker for incomplete unroofing. Observations were conducted using a Total Internal Reflection Fluorescence (TIRF) microscope, as depicted in Figure 2. The observation noted a variance in the quality of the membrane sheets. Additionally, the presence of a nucleus enabled a clear distinction between intact cells and isolated membrane sheets.

3.1.1 Unroofing yield

The efficiency of the two methods was assessed in terms of unroofing yield. The unroofing yield was determined by calculating the percentage of cells that were successfully unroofed out of the total number of cells examined.

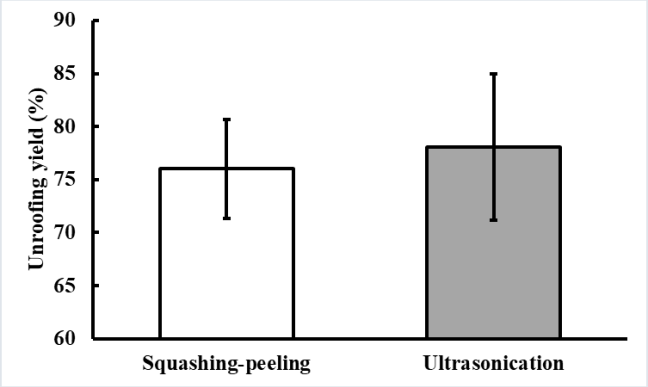

Figure 1. Comparative analysis of unroofing yield. The bar graph depicts the unroofing efficiency between the squashing-peeling method (n=30) and ultrasonication (n=41). The p-value from the t-test is 0.8219, indicating no statistically significant difference between the two methods.

In the preliminary stage of this research, it was observed that the yield of the unroofing process varied between 10% and 40%. However, through practice and optimization, it became feasible to achieve near 100% unroofing

yields using both methods. But the average unroofing yield was slightly higher in ultrasonication than squashing-peeling (figure 1).

3.1.2 Membrane sheet quality assessment

To evaluate the quality of the membranes, two primary criteria were considered: the size of individual membrane sheets and the presence of contaminants such as small, fragmented portions of other membranes. Intact cells exhibited strong membrane staining, and circular nucleus staining. They also appeared slightly blurry. In contrast, membrane sheets showed a weaker membrane signal, no sign of a nucleus, and were confined to a single focal plane under the TIRF angle.

The squashing-peeling presented challenges in terms of manipulation. It had a high risk of the cover slip sliding during peeling. The membranes produced by this method were often unusable due to this error. Similarly, in ultrasonication, the application of ultrasonic frequency induced the movement of the coverslips during the pulses. This problem was mitigated by using a smaller plate but eliminated when the cells were cultured on a MatTek dish. One benefit of the squashing-peeling method is that it can produce both the apical and basal side of the membrane depending on the experimental setup. The ultrasonication-based method was found to be more effective in producing high-quality larger membrane sheets when observed under a TIRF microscope (see Figure 2).

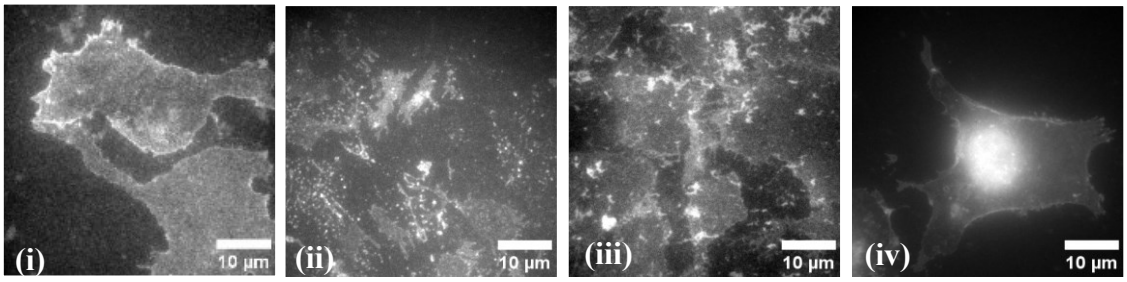

Figure 2. Membrane quality assessment through observation of total internal reflection fluorescence (TIRF) microscopy images of membrane sheets. These sheets were stained with both DAPI and fluorescent WGA conjugate. (i) Large membrane sheet: Two large membrane sheets with clear outlines by WGA staining. It is produced by ultrasonication method. (ii) Small membrane sheets: Multiple smaller membrane sheets, each displaying distinct features. (iii) Contaminated membrane sheets: Membrane sheets with debris, highlighting potential challenges in sample preparation. (iv) Unsuccessful unroofed cell: An intact cell with a remaining nucleus, indicating incomplete unroofing.

3.2 Membrane sheet staining

In conjunction with the utilization of fluorescent WGA conjugate for the staining of membrane sheets, an alternative approach was implemented, involving the transfection of live cells with Caax- Cyan Fluorescent Protein (CFP), succeeded by unroofing and subsequent fixation. The process of Caax-CFP transfection involves introducing a construct into cells that encodes for CFP, which is targeted to cellular membranes by a CAAX motif, thereby labeling the membrane. However, microscopic observation revealed that this technique did not effectively stain the basal membrane. The fluorescence intensity was insufficient, rendering the membrane nearly indistinguishable from the background noise (see Figure 3). Wheat Germ Agglutinin (WGA) fluorescent conjugate staining on live cells before unroofing and fixation yielded marginally improved results (Figure 3). However, the enhancement in staining was still inadequate. This may be due to the possibility that the dye cannot reach the basal membrane efficiently or that the unroofing technique may be contributing to the loss of staining. In contrast, the application of WGA staining post-unroofing, directly on the fixed membrane, demonstrated a marked increase in staining intensity. This produced high-contrast images of the membrane (Figure 3).

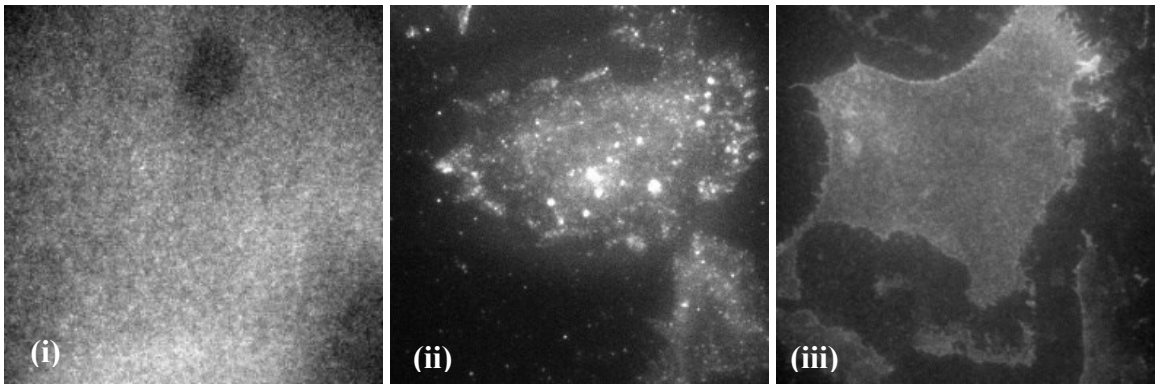

Figure 3: A Comparison of Membrane Staining protocols (i) Transfection with Caax-CFP of live cells Before unroofing results in a faint staining outcome. (ii) Wheat Germ Agglutinin Staining of Live Cells Before Unroofing also results in a faint staining outcome. (iii) Wheat Germ Agglutinin Staining After Unroofing markedly improves the stain intensity.

3.3 Optimization of the ultrasonication unroofing method

An investigation was undertaken to determine the optimal ultrasonication parameters, which included a systematic assessment of temperature, power, and pulse frequency. The findings are presented in Table 2. The best outcomes for membrane quality were achieved at 37°C with 10W power and four pulses, resulting in large, clean membranes. High unroofing yields were observed across all conditions, with a slight reduction to 96.5% when two and four pulses were applied. Membrane quality was notably better at 37°C compared to 4°C, indicating a temperature-sensitive process. A power setting of 10W was more

effective in producing high-quality membranes than 20W and increasing the number of pulses to four improved membrane quality, with a single pulse leading to significant apical membrane contamination and four pulses producing the cleanest membranes with minimal contamination.

Table 2: Impact of Temperature, Power, and Pulse Number on Membrane Quality Post-Ultrasonication

Tested criteria	Ultrasonication parameters							
	Temperature		Power		Number of pulses			
	4 °C	37 °C	10 W	20 W	1	2	3	4
Unroofing yield	100%	100%	100%	100%	100%	96.5%	100%	96.5%
Membrane quality	+	+++	++	+	+	++	++	+++

Note: n=2; Membrane Quality Grading: + = small membranes with contamination; ++ = medium-sized membranes with fewer debris; +++ = large and clean membranes.

3.4 RA reconstitution

The *in vitro* reconstitution of the reticular adhesion complex on isolated membrane sheets necessitated the separate preparation of the membrane sheets and cytosol from two distinct cell types. Membrane sheets were derived from U2OS ITG β5 mScarlet cells, which are characterized by integrin β5 tagged with the fluorescent molecule mScarlet, serving as the membrane sheet donors. In parallel, the cytosol was obtained from U2OS AP2 Halo cells, distinguished by their AP2 proteins tagged with the Halo tag, to facilitate the identification of integrin β5 and AP2 post-reconstitution.

In a control experiment, the membrane sheet was incubated with a buffer solution devoid of cytosolic components. The results demonstrated the presence of integrin β5 on the membrane, yet there was an absence of AP-2 complex sigma subunit signaling, even subsequent to the application of a fluorophore-conjugated halo ligand, indicating that no reconstitution of reticular adhesions occurred in the absence of cytosol. Additionally, immunofluorescent staining for Numb yielded no detectable signal, implying the absence of clathrin-mediated endocytosis (CME) components, as depicted in Figure 4.

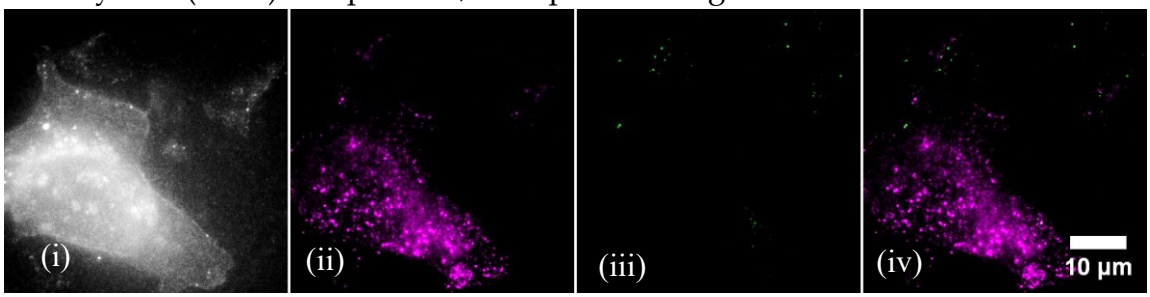

Figure 4: Control experiment on integrin-mediated adhesions by visualization of the membrane without incubation with cytosol. Panel (i) shows Caax-CFP stained membranes; Panel (ii) displays isolated Integrin β5; Panel (iii) lacks AP-2 sigma, staining for Numb; Panel (iv) combines Integrin β5 and Numb, revealing no colocalization.

Following the introduction of cytosol containing halo-tagged AP-2 complex to the membrane sheets and incubation, dispersed clusters of integrin β5 were observed (Figure 5 ii). In rare occasions, spots of AP-2 sigma subunit colocalized with integrin β5 cluster, indicative of reconstituted RAs.

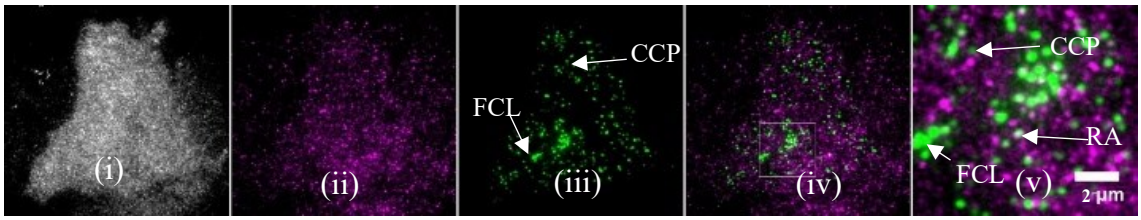

Figure 5: TIRF microscopic examination of membrane sheet post-cytosol incubation for the reconstitution of integrin-based cell-ECM adhesion complexes. Panel (i) illustrates the membrane sheet stained selectively with Caax-CFP. Panel (ii) exhibits Integrin β5 tagged endogenously with the fluorescent protein mScarlet. Panel (iii) shows the AP-2 complex sigma subunit, identified by a Halo tag linked to a fluorophore. The larger AP2 formations are flat clathrin lattices, while the smaller, diffraction-limited formations are identified as clathrin-coated pits. Panel (iv) presents an overlay of Integrin β5 and AP-2 sigma, highlighting their colocalization. Panel (v) provides a magnified view of a specific area from the overlay, distinguishing reticular adhesions, flat clathrin lattices, and clathrin-coated pits by their unique colocalization patterns.

The AP2-sigma-negative integrin β5 clusters were either FAs or pre-FCL immature RAs. The solitary AP2 formation observed was categorized into two distinct types. The first type, characterized by its larger size, was identified as FCLs. The second type, noted for its smaller, diffraction-limited size, was classified as CCPs (Figure 5).

Immunofluorescent staining for FA components (talin1, tensin1, paxillin, FAK, p-FAK, vinculin) allowed to identify the FAs and FXs from non-FA integrin β5 clusters (Figure 6). RAs should not contain talin1, tensin1, paxillin and vinculin. During the limited scope of this experiment, RAs did not demonstrate colocalization with talin1, paxillin, or vinculin. However, colocalization of RAs with tensin1, FAK, and p-FAK was observed on several occasions. It is possible that the tensin-1 colocalization is transient. Additionally, AP-2 sites not associated with integrin β5 were identified as FCLs and CCPs based on their sizes, as shown in Figure 6.

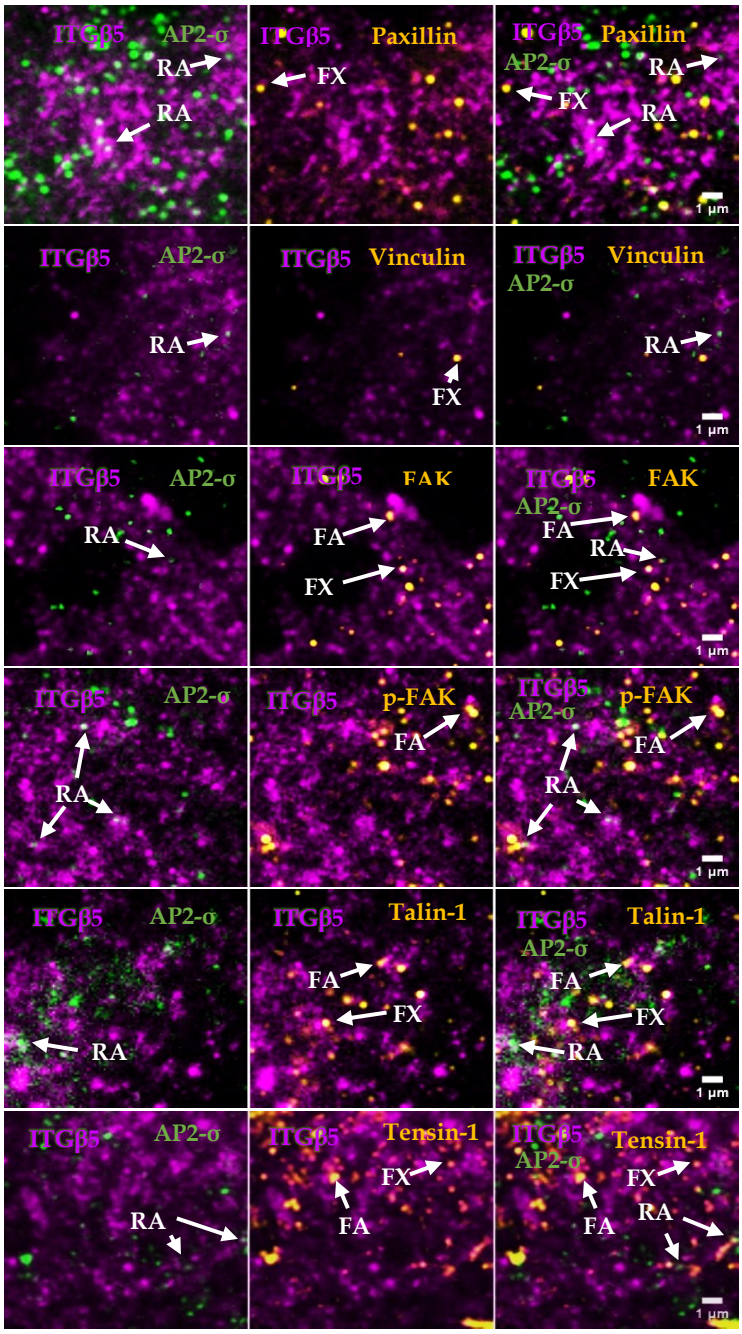

Figure 6. Immunofluorescent characterization of cell-ECM adhesion structures by targeting specific adhesion proteins, such as talin-1, tensin-1, FAK, p-FAK, paxillin, and vinculin. The color of each protein is indicated by the color of its name. The classification of RAs, FAs, and FXs is based on the colocalization of integrin β5 with adhesome components, AP2-σ, and morphological features. Abbreviations: ITGβ5 (Integrin β5), AP2-σ (Adaptor Protein 2 Complex σ Subunit), FAK (Focal Adhesion Kinase), p-FAK (Phosphorylated Focal Adhesion Kinase), RA (Reticular Adhesion), FA (Focal Adhesion), FX (Focal Complex).

3.4 Impact of Incubation Time and Temperature on RA reconstitution

The quantification of the number and dimensions of reticular adhesions (RAs) was achieved through the application of ImageJ software for the analysis of TIRF microscopy images. This analysis was conducted under two experimental conditions: varying temperatures of 4°C and 37°C during a 10-minute incubation period, and varying incubation times of 5, 10, and 20 minutes at a constant temperature of 37°C. The data reveals a higher RA number and increased area size at the higher temperature. The number of RAs exhibited an increase as the incubation time extended, reaching a maximum at 10 minutes. Following this peak, there was a slight decrease in the RA count at 20 minutes. One the other hand, there was a trend of increasing RA size with longer incubation times. The dimensions of RAs were observed to vary, extending from 0.1 μm^2 to 28.90 μm^2, with the average size being calculated at 2.84 μm^2. This experiment indicated temperature and time-dependent dynamics in RA reconstitution.

Table 4 Quantitative analysis of RA number and area across different incubation conditions

	Temperature (10 min incubation)		Incubation period (37 °C temperature)		
	4 °C	37 °C	5 min	10 min	20 min
RA Number	8 9	11 11	2 3	14 14	11 11
Mean	8.5	11	2.5	14	11
RA Area (μm2)	1.50 1.86	2.57 2.88	1.14 3.13	2.57 2.88	5.88 4.04
Mean	1.68	2.72	2.14	2.72	4.96

4 DISCUSSIONS

Among the employed unroofing methods, the squashing-peeling method often compromises the integrity of the membrane sheets. This method involves using a cork to apply pressure and forceps to handle the sample, which can lead to the coverslip sliding due to low friction on the xy-axis and high surface tension in the z-axis between the glass coverslip and the media. This sliding risk can damage the membrane sheet, affect transmembrane proteins, and introduce unwanted cytosolic elements. In contrast, ultrasonication is a reliable method for obtaining larger, intact membrane sheets. Although the squashing-peeling method can be messier and less precise, it is more suitable for cells with higher rigidity. This aligns with previous research, which suggests that cells with greater structural firmness are better handled by this technique (Heuser 2000).

Optimal ultrasonication for cell unroofing was found at 37°C, with 10W power and four pulses, yielding large, clean membranes. Higher temperatures improved membrane integrity, while lower power preserved membrane quality. This combination of temperature, power, and pulses creates an environment where membranes can be cleanly separated with minimal contamination, making them ideal for high-resolution imaging.

In this experiment, the imaging of membrane sheets yielded sufficiently good results. This can be attributed to several factors. Firstly, the use of TIRF microscopy, which produces sharp images by illuminating a thin section of the specimen is suitable for imaging membrane sheets. Secondly, the inherent thinness of the membrane sheets and the absence of cytosol significantly enhanced the fluorescence, allowing light to penetrate with minimal scattering and obviating the need for confocal methods to eliminate out-of-focus light. Additionally, upon analyzing the Caax-CFP transfection method and the fluorescent WGA conjugate staining technique for membrane visualization, it became evident that there were notable differences in their respective effectiveness. The Caax-CFP transfection method, which involves the introduction of a fluorescent protein targeted to plasma membranes, resulted in inadequate staining of the basal membrane. This insufficiency in fluorescence intensity could be attributed to the potential dislodgement of the CFP during the unroofing process. Conversely, the application of fluorescent WGA conjugate staining directly to the fixed membranes after the unroofing procedure significantly improved the staining intensity. This method produced high-contrast images. Therefore, for the most effective visualization of membrane architectures, post-unroofing staining with fluorescent WGA conjugate on fixed membranes is recommended. Furthermore, previous studies have demonstrated that membrane sheets are also advantageous for high-contrast imaging in transmission electron microscopy (TEM), scanning electron microscopy (SEM), and Atomic Force Microscopy (AFM), underscoring their versatility across various microscopy techniques (Nicol and Nermut 1987; Heuser *et al.* 1993; Usukura *et al.* 2016).

The integrin αvβ5 can give rise to either FAs or RAs. The process of RA formation is hypothesized to occur through three different mechanisms. One mechanism involves the frustrated endocytosis of integrin αvβ5 (Zuidema *et al.* 2022; Hakanpää *et al.* 2023). The formation of FCL requires clustering of integrin αvβ5. It has been observed that the formation of RA requires CME machinery. Another proposed mechanism suggests that FCL formation is involved in the recruitment of integrin αvβ5, leading to the formation of stable clusters of integrin αvβ5. There is also evidence supporting this mechanism. A further mechanism suggests a co-assembly of FCLs and integrin αvβ5. There is evidence to suggest that all three of these mechanisms can occur (Hakanpää *et al.* 2023). This experiment has the integrin β5 tagged in the membrane; therefore, it does not study the recruitment of integrin β5 from the cytosol but rather visualizes the clustering of integrin β5 already present in the membrane. Given that the membrane is fluidic and permits the movement of transmembrane proteins, there must be some factors behind the clustering the integrin β5 in the RAs. The observation of some FCLs overlapping with certain αvβ5 regions supports the previously found relationship between the clustering of integrin β5 and the formation of FCLs.

In this study, membrane sheets were used to successfully reconstitute RAs *in vitro*, with TIRF microscopy confirming the recruitment of the AP2 complex to integrin β5. Prior studies have demonstrated that the AP-2 complex interacts with integrins through the intracellular domains of the α and β subunits. Specifically, the NPxY motif on the β5 subunit and the YxxΦ motif on the α subunits are instrumental in guiding the selective engagement with particular integrins (Hemler *et al.* 1992; Deyne *et al.* 1998; Pellinen and Ivaska 2006; Mai *et al.* 2011; De Franceschi *et al.* 2016). In cells located in low tension regions, integrin β5 preferentially binds to ARH and Numb adaptor proteins over talin 1, clustering within flat clathrin structures. All three of these proteins interact with the NPxY motif. Lack of actomyosin activity promotes this clustering of integrin β5 and it likely involves phosphorylation of a specific site in the β5 subunit. Additional proteins like Rho guanine nucleotide exchange factors and microtubule affinity regulating kinase 2 are crucial for this clustering to occur (Zuidema *et al.* 2018).

Conversely, the AP-2 complex's β chain is known to be critical in forming the clathrin lattice by linking to ECM-bound receptors (Shih *et al.* 1995; Yu *et al.* 2015). Proteins like Dab2 and ARH may displace integrin from actin connections (Caswell *et al.* 2007; Ezratty *et al.* 2009). This may promote αVβ5 clustering by the AP-2 complex into RAs. The stability of integrin β5 cluster at RA sites, even subsequent to the removal of other proteins, can be assessed through the application of elastase to RA-enriched membrane sheets that have been reconstituted, as outlined in a previous study (Peeler *et al.* 1993b).

In this study, the membrane sheets reconstituted with RAs were subjected to immunofluorescence staining for tensin1, FAK, p-FAK, paxillin, talin1, and vinculin to assess the presence of these focal adhesion components. FA proteins like tensin1, FAK, and p-FAK occasionally colocalize with reticular adhesions (RAs). However, their consistent presence in RAs is uncertain from the limited sample size and the nature of this experiment. Tensin1 is a component of fibrillar adhesions essential for fibronectin matrix formation, interacts with the actin cytoskeleton (Lo *et al.* 1994; Pankov *et al.* 2000). It interacts with kinases associated with focal adhesions, including FAK, via its Src homology 2 (SH2) domain (Davis *et al.* 1991). Tensin1 should not be present in RAs and may be transient. Literature suggests that FAK, a tyrosine kinase that binds to the β subunit of integrin, plays a significant role in RA assembly. Upon phosphorylation at tyrosine residue 861, FAK interacts more with the cytoplasmic side of αVβ5 integrin receptors (Schaller *et al.* 1995; Eliceiri *et al.* 2002). It was found in a previous study that both FAK and p-FAK are involved in RA assembly in retinal pigment epithelial cells, maintaining their connection with the interphotoreceptor matrix and photoreceptor outer segments (Nandrot *et al.* 2004; Lock *et al.* 2019).

Previous studies indicate that RAs do not colocalize with talin1 or paxillin and are vinculin-negative (Giancotti 2000; Calderwood *et al.* 2002; Lock *et al.* 2018). Vinculin, a mechano-coupling protein, and talin1, which can directly bind to integrins, are involved in linking the extracellular environment to the actomyosin cytoskeleton (Mierke *et al.* 2008; Zhang *et al.* 2008). In our observations, these components also did not colocalize with RA sites.

The experimental findings regarding reticular adhesions (RAs) reveal that both temperature and time are pivotal in their development and structure. The change in the number and size of RAs at an elevated temperature of 37°C indicates that RAs are thermally sensitive, with higher temperatures promoting larger adhesion formation. Lower temperatures can result in slower biochemical reactions, which are essential for the assembly and maturation of reticular adhesions. Additionally, the physical properties of the ECM, which play a crucial role in reticular adhesion dynamics, may be altered at lower temperatures, affecting the optimal mechanical forces necessary for reticular adhesion development (Sun 2021). This can lead to a slower rate of reticular adhesion maturation.

This research employed a PLL-coated glass substrate to reconstitute RAs, demonstrating their potential to form on rigid surfaces. But it is also true that cells can also alter the ECM to meet their adhesion requirements by synthesizing and secreting ECM molecules (Geiger and Yamada 2011). The relationship between matrix stiffness and RA regulation is not fully understood. Research suggests that excessive stiffness may cause rapid force transmission, leading to the premature release of FA proteins and hindering the recruitment of additional FA proteins necessary for force distribution. This could result in 'frictional slippage,' impacting cell movement and adhesion (Adebowale *et al.* 2021). Future studies might explore this using a tunable elastic hydrogel matrix to find the ideal

stiffness for RA formation and to understand its influence on RA clustering (Deng *et al.* 2023). Moreover, increased ECM rigidity has been linked to enhanced cell cycle progression and tumor growth, suggesting that substrate stiffness studies could offer valuable therapeutic insights (Aragona *et al.* 2013; Pickup *et al.* 2014). Just as the stiffness of the ECM influences cellular behavior, cells exert forces on the ECM through adhesion sites, with traction force measurements providing insight into the adhesion complexes' mechanical properties. Two main methods to assess these forces are traction force microscopy, which calculates force vectors from the displacement of markers within a substrate (Zielinski *et al.* 2013), and the use of microfabricated structures like nanopillar arrays to directly measure forces at adhesion points (Saez *et al.* 2010; Kuo *et al.* 2010).

This experiment only dealt with the assembly of RA and not its disassembly. There is scope for performing an *in vitro* disassembly study of RAs. Studies suggest that RAs have the potential to develop into FAs (Zuidema *et al.* 2018; Lukas *et al.* 2024). The membrane sheets utilized in these experiments, along with the reconstitution and monitoring of RA transformations on them, could serve as valuable tools for future research in this domain. Previous studies show that the enzyme type I phosphatidylinositol phosphate kinase (PIPKIγ), activated by FAK interactions, plays a crucial role in the disassembly of FA (Ling *et al.* 2002) by disrupting talin-integrin connections (Barsukov *et al.* 2003). During recycling, clathrin and its adaptors, such as Dab2 and ARH, target the adhesions, with mature FAs showing increased tyrosine phosphorylation that facilitates CME (Chao and Kunz 2009; Ezratty *et al.* 2009; Batchelder and Yarar 2010). Interestingly, integrin αVβ5 alters this process by preventing the formation of clathrin-coated pits, resulting in flat clathrin lattices (Smilenov *et al.* 1999; Baschieri *et al.* 2018). There is evidence of RA-like structure to also undergo disassembly and endocytosis by the CME process (Lampe *et al.* 2016). While actin polymerization is not always necessary for CCP formation, it becomes crucial in membrane invagination and scission during CME (Saffarian *et al.* 2009). During RA endocytosis, the clathrin in these pits often originates from preexisting FCLs rather than new recruitment (Sochacki and Taraska 2019). However, the endocytosis of RAs is still a mystery.

The technique of *in vitro* reconstitution of reticular adhesions (RAs) provides us the capability to precisely manipulate and observe the detailed processes involved in the formation and functionality of RAs within controlled conditions. Although *in vitro* experiments have significantly advanced our knowledge of cell-ECM adhesions, but they fall short of replicating the transient nature of cell-ECM adhesions. For example, FA-like structures observed *in vivo* are typically smaller than *in vitro* (Yamaguchi and Knaut 2022). This highlights the need for experimental models that better reflect the living cellular environment. To deepen our understanding of RAs, research must explore their potential reconstitution in a soft 3D ECM, which could reveal differences in their formation and function compared to 2D models. The identification of curved adhesions within a 3D ECM underscores this need, as these structures, mediated

by integrin αVβ5 and distinct from FAs and RAs, lack clathrin and include specific adhesion proteins like zyxin (Zhang *et al.* 2023). While it may still be a distant prospect, the development of a three-dimensional synthetic cell model, complete with an artificial cytoskeleton and components of reticular adhesions (RAs), could provide a more precise platform for exploring the function of RAs in cell migration (Sauter *et al.* 2023).

Advanced imaging technologies could be integrated with *in vitro* RA models to visualize adhesion dynamics in real-time, providing a more detailed view of these processes. The incorporation of microfluidic platforms could mimic the *in vivo* microenvironment more closely, allowing for the study of RAs under physiological flow conditions. Computational tools can be developed to simulate RA behavior, offering predictive models that can guide experimental design and interpretation. *In vitro* reconstitution of RAs should enable high-throughput screening for modulators of RA dynamics, aiding drug discovery and the development of targeted therapies. Such studies are crucial for preclinical testing of new drugs, understanding cellular processes in disease, and potentially identifying biomarkers for diagnostics and advancing tissue engineering by controlling cell adhesion.

In conclusion, the *in vitro* reconstitution of RAs holds great promise for the future, with the potential to bridge gaps in our understanding of RA biology and translate these findings into tangible medical advancements. As we continue to explore the molecular landscape of RAs, we can expect to uncover novel insights that will shape the future of cell biology and medicine.

ACKNOWLEDGEMENTS

In the beginning, I humbly express my gratitude to The All-knowing, for the strength and wisdom bestowed upon me during this academic pursuit.

I am deeply grateful to my supervisor, Dr. Leonardo Almeida-Souza, for his invaluable guidance and inspiration throughout my project. His mentorship, encouragement for independent problem-solving, and insightful stories from cell biology have greatly enriched my academic experience. Despite his busy schedule, Leonardo's dedication and passion for thorough research have been instrumental in my progress.

My sincere appreciation goes to my home institution supervisor, Professor Janne Ihalainen, for his guidance through the thesis project searching journey. His lookout for my well-being throughout the thesis journey, along with his feedback and overall support, have been fundamental to my success.

I want to thank my university, the University of Jyväskylä for allowing me to do a master's in nanoscience and making it possible to do this research work. I want to thank the endocytic cytoskeleton biology group of the University of Helsinki for supporting me financially during the time of my project work.

Special gratitude is extended to my colleague and mentor, Dr. Laura Hakanpää, for teaching me the practical aspects of our work. Laura's help in familiarizing me with the laboratory, clearing my confusion, guiding me through the project work, interpreting the results, and providing feedback has been crucial in my learning process.

I am also grateful to my colleagues An-Sofie Lenaerts, Seyda Culfa, Narjes Zeinoddin, and Dr. Jekaterina Kristal for their assistance and shared expertise throughout this journey.

Overall, I am profoundly grateful for all the guidance and support I have received throughout my research journey, which has been instrumental in the completion of this thesis.

Vantaa May 24, 2024
Mohammed Mostafa Al Quadir

REFERENCES

Abercrombie M. 1980. The Croonian Lecture, 1978: The Crawling Movement of Metazoan Cells. *Proceedings of the Royal Society of London. Series B, Biological Sciences*: 129–147.

Abercrombie M. & Dunn G.A. 1975. Adhesions of fibroblasts to substratum during contact inhibition observed by interference reflection microscopy. *Experimental Cell Research* 92: 57–62.

Abercrombie M. & Heaysman J.E.M. 1953. Observations on the social behaviour of cells in tissue culture. *Experimental Cell Research* 5: 111–131.

Abercrombie M., Heaysman J.E.M. & Pegrum S.M. 1971. The locomotion of fibroblasts in culture. *Experimental Cell Research* 67: 359–367.

Adebowale K., Gong Z., Hou J.C., Wisdom K.M., Garbett D., Lee H., Nam S., Meyer T., Odde D.J., Shenoy V.B. & Chaudhuri O. 2021. Enhanced substrate stress relaxation promotes filopodia-mediated cell migration. *Nature Materials* 20: 1290–1299.

Akisaka T., Yoshida H., Suzuki R. & Takama K. 2008. Adhesion structures and their cytoskeleton-membrane interactions at podosomes of osteoclasts in culture. *Cell and Tissue Research* 331: 625–641.

Akiyama S.K., Olden K. & Yamada K.M. 1995. Fibronectin and integrins in invasion and metastasis. *Cancer and Metastasis Reviews* 14: 173–189.

Akiyama S.K. & Yamada K.M. 1985. Synthetic peptides competitively inhibit both direct binding to fibroblasts and functional biological assays for the purified cell-binding domain of fibronectin. *Journal of Biological Chemistry* 260: 10402–10405.

Alfonzo-Méndez M.A., Sochacki K.A., Strub M.-P. & Taraska J.W. 2022. Dual clathrin and integrin signaling systems regulate growth factor receptor activation. *Nature Communications* 13: 905.

Aragona M., Panciera T., Manfrin A., Giulitti S., Michielin F., Elvassore N., Dupont S. & Piccolo S. 2013. A Mechanical Checkpoint Controls

Multicellular Growth through YAP/TAZ Regulation by Actin-Processing Factors. *Cell* 154: 1047–1059.

Bachir A.I., Zareno J., Moissoglu K., Plow E.F., Gratton E. & Horwitz A.R. 2014. Integrin-Associated Complexes Form Hierarchically with Variable Stoichiometry in Nascent Adhesions. *Current Biology* 24: 1845–1853.

Barlowe C. 1994. COPII: A membrane coat formed by Sec proteins that drive vesicle budding from the endoplasmic reticulum. *Cell* 77: 895–907.

Barsukov I.L., Prescot A., Bate N., Patel B., Floyd D.N., Bhanji N., Bagshaw C.R., Letinic K., Paolo G. Di, Camilli P. De, Roberts G.C.K. & Critchley D.R. 2003. Phosphatidylinositol Phosphate Kinase Type 1γ and β1-Integrin Cytoplasmic Domain Bind to the Same Region in the Talin FERM Domain. *Journal of Biological Chemistry* 278: 31202–31209.

Baschieri F., Dayot S., Elkhatib N., Ly N., Capmany A., Schauer K., Betz T., Vignjevic D.M., Poincloux R. & Montagnac G. 2018. Frustrated endocytosis controls contractility-independent mechanotransduction at clathrin-coated structures. *Nature Communications* 9: 3825.

Baschieri F., Porshneva K. & Montagnac G. 2020. Frustrated clathrin-mediated endocytosis – causes and possible functions. *Journal of Cell Science* 133.

Batchelder E.M. & Yarar D. 2010. Differential Requirements for Clathrin-dependent Endocytosis at Sites of Cell–Substrate Adhesion. *Molecular Biology of the Cell* 21: 3070–3079.

Berrier A.L. & Yamada K.M. 2007. Cell–matrix adhesion. *Journal of Cellular Physiology* 213: 565–573.

Bertolotti R., Rutishauser U. & Edelman G.M. 1980. A cell surface molecule involved in aggregation of embryonic liver cells. *Proceedings of the National Academy of Sciences* 77: 4831–4835.

Bock G., Goode J., Foundation N. & Biology S. on the L. of R. in. 1998. *The Limits of Reductionism in Biology*. Wiley.

Boucrot E., Saffarian S., Zhang R. & Kirchhausen T. 2010. Roles of AP-2 in Clathrin-Mediated Endocytosis. *PLoS ONE* 5: e10597.

Burridge K. & Connell L. 1983. Talin: A cytoskeletal component concentrated in adhesion plaques and other sites of actin-membrane interaction. *Cell Motility* 3: 405–417.

Burridge K., Fath K., Kelly T., Nuckolls G. & Turner C. 1988. Focal adhesions: Transmembrane junctions between the extracellular matrix and the cytoskeleton. *Annual Review of Cell Biology* 4: 487–525.

Calderwood D.A., Yan B., Pereda J.M. de, Alvarez B.G., Fujioka Y., Liddington R.C. & Ginsberg M.H. 2002. The Phosphotyrosine Binding-like Domain of Talin Activates Integrins. *Journal of Biological Chemistry* 277: 21749–21758.

Caswell P.T., Spence H.J., Parsons M., White D.P., Clark K., Cheng K.W., Mills G.B., Humphries M.J., Messent A.J., Anderson K.I., McCaffrey M.W., Ozanne B.W. & Norman J.C. 2007. Rab25 Associates with α5β1 Integrin to Promote Invasive Migration in 3D Microenvironments. *Developmental Cell* 13: 496–510.

Chao W.-T. & Kunz J. 2009. Focal adhesion disassembly requires clathrin-dependent endocytosis of integrins. *FEBS Letters* 583: 1337–1343.

Chastney M.R., Conway J.R.W. & Ivaska J. 2021. Integrin adhesion complexes. *Current Biology* 31: R536–R542.

Cheresh D.A., Smith J.W., Cooper H.M. & Quaranta V. 1989. A Novel Vitronectin Receptor lntegrin (avP,J Is Responsible for Distinct Adhesive Properties of Carcinoma Cells. *Cell* 57: 59–69.

Chrzanowska-Wodnicka M. & Burridge K. 1996. Rho-stimulated contractility drives the formation of stress fibers and focal adhesions. *The Journal of cell biology* 133: 1403–1415.

Cukier I.H., Li Y. & Lee J.M. 2007. Cyclin B1/Cdk1 binds and phosphorylates Filamin A and regulates its ability to cross-link actin. *FEBS Letters* 581: 1661–1672.

Cukierman E., Pankov R., Stevens D.R. & Yamada K.M. 2001. Taking Cell-Matrix Adhesions to the Third Dimension. *Science* 294: 1708–1712.

Curtis A.S.G. 1964. The mechanism of adhesion of cells to glass. *The Journal of Cell Biology* 20: 199–215.

Davis S., Lu M.L., Lo S.H., Lin S., Butler J.A., Druker B.J., Roberts T.M., An Q. & Chen L.B. 1991. Presence of an SH2 Domain in the Actin-Binding Protein Tensin. *Science* 252: 712–715.

Deng H., Shu X., Wang Y., Zhang J., Yin Y., Wu F. & He J. 2023. Matrix Stiffness Regulated Endoplasmic Reticulum Stress-mediated Apoptosis of Osteosarcoma Cell through Ras Signal Cascades. *Cell Biochemistry and Biophysics* 81: 839–850.

Deyne P.G. De, O'Neill A., Resneck W.G., Dmytrenko G.M., Pumplin D.W. & Bloch R.J. 1998. The vitronectin receptor associates with clathrin-coated membrane domains via the cytoplasmic domain of its β5 subunit. *Journal of Cell Science* 111: 2729–2740.

Duval K., Grover H., Han L.-H., Mou Y., Pegoraro A.F., Fredberg J. & Chen Z. 2017. Modeling Physiological Events in 2D vs. 3D Cell Culture. *Physiology* 32: 266–277.

Eliceiri B.P., Puente X.S., Hood J.D., Stupack D.G., Schlaepfer D.D., Huang X.Z., Sheppard D. & Cheresh D.A. 2002. Src-mediated coupling of focal adhesion kinase to integrin **α** v **β** 5 in vascular endothelial growth factor signaling. *The Journal of Cell Biology* 157: 149–160.

Elkhatib N., Porshneva K. & Montagnac G. 2021. Migration cues interpretation by clathrin-coated structures. *Current Opinion in Cell Biology* 72: 100–105.

Ezratty E.J., Bertaux C., Marcantonio E.E. & Gundersen G.G. 2009. Clathrin mediates integrin endocytosis for focal adhesion disassembly in migrating cells. *Journal of Cell Biology* 187: 733–747.

Fededa J.P. & Gerlich D.W. 2012. Molecular control of animal cell cytokinesis. *Nature Cell Biology* 14: 440–447.

Fish K.N. 2009. Total Internal Reflection Fluorescence (TIRF) Microscopy. *Current Protocols in Cytometry* 50.

Flinn H.M. & Ridley A.J. 1996. Rho stimulates tyrosine phosphorylation of focal adhesion kinase, p130 and paxillin. *Journal of Cell Science* 109: 1133–1141.

Franceschi N. De, Arjonen A., Elkhatib N., Denessiouk K., Wrobel A.G., Wilson T.A., Pouwels J., Montagnac G., Owen D.J. & Ivaska J. 2016. Selective integrin endocytosis is driven by interactions between the integrin α-chain and AP2. *Nature Structural & Molecular Biology* 23: 172–179.

Frantz C., Stewart K., science V.W.-J. of cell & 2010 undefined. 2010. The extracellular matrix at a glance. *journals.biologists.comC Frantz, KM Stewart, VM WeaverJournal of cell science, 2010•journals.biologists.com* 123: 4195–4200.

Garcia J.G.N., Verin A.D., Schaphorst K., Siddiqui R., Patterson C.E., Csortos C. & Natarajan V. 1999. Regulation of endothelial cell myosin light chain kinase by Rho, cortactin, and p60 ^{src}. *American Journal of Physiology-Lung Cellular and Molecular Physiology* 276: L989–L998.

Geiger B. 1979. A 130K protein from chicken gizzard: Its localization at the termini of microfilament bundles in cultured chicken cells. *Cell* 18: 193–205.

Geiger B. & Yamada K.M. 2011. Molecular Architecture and Function of Matrix Adhesions. *Cold Spring Harbor Perspectives in Biology* 3: a005033–a005033.

Geiger T. & Zaidel-Bar R. 2012. Opening the floodgates: proteomics and the integrin adhesome. *Current Opinion in Cell Biology* 24: 562–568.

Getzoff E.D., Tainer J.A., Weiner P.K., Koilman P.A., Richardson J.S., Richardson D.C., Allison A., Bacquet R.J., McCammon J.A., press in, Beem K.M., Allison S.A., Lau W.F., Lybrand T.P., Mazor M.H., Nortrup S.H., Pettitt B.M., Wong S A Allison C.F., Honig B., KolUman P.A., Northrup S.H., Erkki Ruoslahti I. & Pierschbacher M.D. 1987. New Perspectives in Cell Adhesion: RGD and Integrins. *Science* 238: 491–497.

Giancotti F.G. 2000. Complexity and specificity of integrin signalling. *Nature Cell Biology* 2: E13–E14.

Grobstein C. & Parker G. 1954. In vitro Induction of Cartilage in Mouse Somite Mesoderm by Embryonic Spinal Cord. *Experimental Biology and Medicine* 85: 477–481.

Grove J., Metcalf D.J., Knight A.E., Wavre-Shapton S.T., Sun T., Protonotarios E.D., Griffin L.D., Lippincott-Schwartz J. & Marsh M. 2014. Flat clathrin lattices: Stable features of the plasma membrane. *Molecular Biology of the Cell* 25: 3581–3594.

Hakanpää L., Abouelezz A., Lenaerts A.-S., Culfa S., Algie M., Bärlund J., Katajisto P., McMahon H. & Almeida-Souza L. 2023. Reticular adhesions are assembled at flat clathrin lattices and opposed by active integrin α5β1. *Journal of Cell Biology* 222.

Harris A. 1973. Location of cellular adhesions to solid substrata. *Developmental Biology* 35: 97–114.

Harrison R.G. 1906. Observations on the living developing nerve fiber. *Experimental Biology and Medicine* 4: 140–143.

He K., Sakai T., Tsukasaki Y., Watanabe T.M. & Ikebe M. 2017. Myosin X is recruited to nascent focal adhesions at the leading edge and induces multi-cycle filopodial elongation. *Scientific Reports* 7: 13685.

Heath J.P. & Dunn G.A. 1978. Cell to substratum contacts of chick fibroblasts and their relation to the microfilament system. a correlated interference-reflexion and high-voltage electron-microscope study. *Journal of Cell Science* 29: 197–212.

Hemler M.E., Kassner P.D. & Chan B.M.C. 1992. Functional Roles for Integrin Subunit Cytoplasmic Domains. *Cold Spring Harbor Symposia on Quantitative Biology* 57: 213–220.

Heuser J. 2000. The production of'cell cortices' for light and electron microscopy. *Traffic (Copenhagen, Denmark)* 1: 545–552.

Heuser J. & Evans L. 1980. Three-dimensional visualization of coated vesicle formation in fibroblasts. *Journal of Cell Biology* 84: 560–583.

Heuser J., Zhu Q. & Clarke M. 1993. Proton pumps populate the contractile vacuoles of Dictyostelium amoebae. *The Journal of cell biology* 121: 1311–1327.

Högnäs G., Tuomi S., Veltel S., Mattila E., Murumägi A., Edgren H., Kallioniemi O. & Ivaska J. 2012. Cytokinesis failure due to derailed integrin traffic induces aneuploidy and oncogenic transformation in vitro and in vivo. *Oncogene* 31: 3597–3606.

Hynes R.O. 1987. Integrins: A family of cell surface receptors. *Cell* 48: 549–554.

Hynes R.O. 2002. Integrins: Bidirectional, allosteric signaling machines. *Cell* 110: 673–687.

Hynes R.O. & Destree A.T. 1978. Relationships between fibronectin (LETS protein) and actin. *Cell* 15: 875–886.

Izzard C.S. & Lochner L.R. 1976. Cell-to-substrate contacts in living fibroblasts: an interference reflexion study with an evaluation of the technique. *Journal of Cell Science* 21: 129–159.

Jones M.C., Askari J.A., Humphries J.D. & Humphries M.J. 2018. Cell adhesion is regulated by CDK1 during the cell cycle. *Journal of Cell Biology* 217: 3203–3218.

Kaksonen M. & Roux A. 2018. Mechanisms of clathrin-mediated endocytosis. *Nature Reviews Molecular Cell Biology* 19: 313–326.

Kamranvar S.A., Gupta D.K., Wasberg A., Liu L., Roig J. & Johansson S. 2022. Integrin-Mediated Adhesion Promotes Centrosome Separation in Early Mitosis. *Cells* 11: 1360.

Kanchanawong P. & Calderwood D.A. 2023. Organization, dynamics and mechanoregulation of integrin-mediated cell–ECM adhesions. *Nature Reviews Molecular Cell Biology* 24: 142–161.

Kuo C., Shiu J., Chien F., Tsai S., Chueh D. & Chen P. 2010. Polymeric nanopillar arrays for cell traction force measurements. *Electrophoresis* 31: 3152–3158.

Lampe M., Vassilopoulos S. & Merrifield C. 2016. Clathrin coated pits, plaques and adhesion. *Journal of Structural Biology* 196: 48–56.

Lancaster O.M., Le Berre M., Dimitracopoulos A., Bonazzi D., Zlotek-Zlotkiewicz E., Picone R., Duke T., Piel M. & Baum B. 2013. Mitotic Rounding Alters Cell Geometry to Ensure Efficient Bipolar Spindle Formation. *Developmental Cell* 25: 270–283.

Laukaitis C.M., Webb D.J., Donais K. & Horwitz A.F. 2001. Differential Dynamics of α5 Integrin, Paxillin, and α-Actinin during Formation and Disassembly of Adhesions in Migrating Cells. *The Journal of Cell Biology* 153: 1427–1440.

Lazarides E. & Burridge K. 1975. α-Actinin: Immunofluorescent localization of a muscle structural protein in nonmuscle cells. *Cell* 6: 289–298.

Lazarides E. & Weber K. 1974. Actin Antibody: The Specific Visualization of Actin Filaments in Non-Muscle Cells. *Proceedings of the National Academy of Sciences* 71: 2268–2272.

Legate K.R., Wickström S.A. & Fässler R. 2009. Genetic and cell biological analysis of integrin outside-in signaling. *Genes & Development* 23: 397–418.

Lehman I.R., Bessman M.J., Simms E.S. & Kornberg A. 1958. Enzymatic Synthesis of Deoxyribonucleic Acid. *Journal of Biological Chemistry* 233: 163–170.

Lewis W.H. 1922. The adhesive quality of cells. *The Anatomical Record* 23: 387–392.

Leyton-Puig D., Isogai T., Argenzio E., Broek B. van den, Klarenbeek J., Janssen H., Jalink K. & Innocenti M. 2017. Flat clathrin lattices are dynamic actin-controlled hubs for clathrin-mediated endocytosis and signalling of specific receptors. *Nature Communications* 8: 16068.

Li J., Jung W., Nam S., Chaudhuri O. & Kim T. 2020. Roles of Interactions Between Cells and Extracellular Matrices for Cell Migration and Matrix Remodeling. In: pp. 247–282.

Linder S. 2007. The matrix corroded: podosomes and invadopodia in extracellular matrix degradation. *Trends in Cell Biology* 17: 107–117.

Linder S. 2009. Invadosomes at a glance. *Journal of Cell Science* 122: 3009–3013.

Ling K., Doughman R.L., Firestone A.J., Bunce M.W. & Anderson R.A. 2002. Type Iγ phosphatidylinositol phosphate kinase targets and regulates focal adhesions. *Nature* 420: 89–93.

Liu A.P. & Fletcher D.A. 2009. Biology under construction: in vitro reconstitution of cellular function. *Nature Reviews Molecular Cell Biology* 10: 644–650.

Lo S.H., Janmey P.A., Hartwig J.H. & Chen L.B. 1994. Interactions of tensin with actin and identification of its three distinct actin-binding domains. *The Journal of cell biology* 125: 1067–1075.

Lock J.G., Baschieri F., Jones M.C., Humphries J.D., Montagnac G., Strömblad S. & Humphries M.J. 2019. Clathrin-containing adhesion complexes. *Journal of Cell Biology* 218: 2086–2095.

Lock J.G., Jones M.C., Askari J.A., Gong X., Oddone A., Olofsson H., Göransson S., Lakadamyali M., Humphries M.J. & Strömblad S. 2018. Reticular adhesions are a distinct class of cell-matrix adhesions that mediate attachment during mitosis. *Nature Cell Biology* 20: 1290–1302.

Lock J.G., Wehrle-Haller B. & Strömblad S. 2008. Cell–matrix adhesion complexes: Master control machinery of cell migration. *Seminars in Cancer Biology* 18: 65–76.

Lukas F., Matthaeus C., López-Hernández T., Lahmann I., Schultz N., Lehmann M., Puchkov D., Pielage J., Haucke V. & Maritzen T. 2024. Canonical and non-canonical integrin-based adhesions dynamically interconvert. *Nature Communications* 15: 2093.

Mai A., Veltel S., Pellinen T., Padzik A., Coffey E., Marjomäki V. & Ivaska J. 2011. Competitive binding of Rab21 and p120RasGAP to integrins regulates receptor traffic and migration. *Journal of Cell Biology* 194: 291–306.

Maritzen T., Schachtner H. & Legler D.F. 2015. On the move: endocytic trafficking in cell migration. *Cellular and Molecular Life Sciences* 72: 2119–2134.

McMahon H.T. & Boucrot E. 2011. Molecular mechanism and physiological functions of clathrin-mediated endocytosis. *Nature Reviews Molecular Cell Biology* 12: 517–533.

Mierke C.T., Kollmannsberger P., Paranhos Zitterbart D., Smith J., Fabry B. & Goldmann W.H. 2008. Mechano-Coupling and Regulation of Contractility by the Vinculin Tail Domain. *Biophysical Journal* 94: 661–670.

Mishra Y.G. & Manavathi B. 2021. Focal adhesion dynamics in cellular function and disease. *Cellular Signalling* 85: 110046.

Morgan M.R., Humphries M.J. & Bass M.D. 2007. Synergistic control of cell adhesion by integrins and syndecans. *Nature Reviews Molecular Cell Biology* 8: 957–969.

Mousa S.A. 2008. Cell Adhesion Molecules: Potential Therapeutic & Diagnostic Implications. *Molecular Biotechnology* 38: 33–40.

Müller K. & Gerisch G. 1978. A specific glycoprotein as the target site of adhesion blocking Fab in aggregating Dictyostelium cells. *Nature* 274: 445–449.

Nandrot E.F., Kim Y., Brodie S.E., Huang X., Sheppard D. & Finnemann S.C. 2004. Loss of Synchronized Retinal Phagocytosis and Age-related Blindness in Mice Lacking αvβ5 Integrin. *The Journal of Experimental Medicine* 200: 1539–1545.

Nermut M. V. 1982. The" cell monolayer technique" in membrane research.

Nicol A. & Nermut M. V. 1987. A new type of substratum adhesion structure in NRK cells revealed by correlated interference reflection and electron microscopy. *European journal of cell biology* 43: 348–357.

Nishimura T. & Kaibuchi K. 2007. Numb Controls Integrin Endocytosis for Directional Cell Migration with aPKC and PAR-3. *Developmental Cell* 13: 15–28.

Nolte M.A., Nolte-'t Hoen E.N.M. & Margadant C. 2021. Integrins Control Vesicular Trafficking; New Tricks for Old Dogs. *Trends in Biochemical Sciences* 46: 124–137.

Nurse P. 2007. Reductionism and Explanation in Cell Biology. In: *Novartis Foundation Symposium 213*, pp. 93–105.

Oakes P.W., Bidone T.C., Beckham Y., Skeeters A. V., Ramirez-San Juan G.R., Winter S.P., Voth G.A. & Gardel M.L. 2018. Lamellipodium is a myosin-independent mechanosensor. *Proceedings of the National Academy of Sciences* 115: 2646–2651.

Pankov R., Cukierman E., Katz B.-Z., Matsumoto K., Lin D.C., Lin S., Hahn C. & Yamada K.M. 2000. Integrin Dynamics and Matrix Assembly. *The Journal of Cell Biology* 148: 1075–1090.

Parsons J.T., Horwitz A.R. & Schwartz M.A. 2010. Cell adhesion: integrating cytoskeletal dynamics and cellular tension. *Nature Reviews Molecular Cell Biology* 11: 633–643.

Pascalis C. De & Etienne-Manneville S. 2017. Single and collective cell migration: the mechanics of adhesions. *Molecular Biology of the Cell* 28: 1833–1846.

Pearse B.M.F. 1976. Clathrin: A unique protein associated with intracellular transfer of membrane by coated vesicles. *Proceedings of the National Academy of Sciences of the United States of America* 73: 1255–1259.

Peeler J.S., Donzell W.C. & Anderson R.G. 1993a. The appendage domain of the AP-2 subunit is not required for assembly or invagination of clathrin-coated pits. *The Journal of cell biology* 120: 47–54.

Peeler J.S., Donzell W.C. & Anderson R.G. 1993b. The appendage domain of the AP-2 subunit is not required for assembly or invagination of clathrin-coated pits. *The Journal of cell biology* 120: 47–54.

Pellinen T. & Ivaska J. 2006. Integrin traffic. *Journal of Cell Science* 119: 3723–3731.

Pickup M.W., Mouw J.K. & Weaver V.M. 2014. The extracellular matrix modulates the hallmarks of cancer. *EMBO reports* 15: 1243–1253.

Reilein A. & Nelson W.J. 2005. APC is a component of an organizing template for cortical microtubule networks. *Nature Cell Biology* 7: 463–473.

Reinhard M., Giehl K., Abel K., Haffner C., Jarchau T., Hoppe V., Jockusch B.M. & Walter U. 1995. The proline-rich focal adhesion and microfilament protein VASP is a ligand for profilins. *The EMBO Journal* 14: 1583–1589.

Ruoslahti E., Hayman E.G. & Pierschbacher M.D. 1985. Extracellular matrices and cell adhesion. *Arteriosclerosis* 5: 581–594.

Rutishauser U., Thiery J.P., Brackenbury R. & Edelman G.M. 1978. Adhesion among neural cells of the chick embryo. III. Relationship of the surface molecule CAM to cell adhesion and the development of histotypic patterns. *The Journal of cell biology* 79: 371–381.

Saez A., Anon E., Ghibaudo M., Roure O. du, Meglio J.-M. Di, Hersen P., Silberzan P., Buguin A. & Ladoux B. 2010. Traction forces exerted by epithelial cell sheets. *Journal of Physics: Condensed Matter* 22: 194119.

Saffarian S., Cocucci E. & Kirchhausen T. 2009. Distinct Dynamics of Endocytic Clathrin-Coated Pits and Coated Plaques. *PLoS Biology* 7: e1000191.

Sauter D., Schröter M., Frey C., Weber C., Mersdorf U., Janiesch J., Platzman I. & Spatz J.P. 2023. Artificial Cytoskeleton Assembly for Synthetic Cell Motility. *Macromolecular Bioscience* 23.

Schaller M.D., Otey C.A., Hildebrand J.D. & Parsons J.T. 1995. Focal adhesion kinase and paxillin bind to peptides mimicking beta integrin cytoplasmic domains. *The Journal of cell biology* 130: 1181–1187.

Schmid S.L. 1997. Clathrin-coated vesicle formation and protein sorting: An Integrated Process. *Annual Review of Biochemistry* 66: 511–548.

Sheetz M.P., Felsenfeld D.P. & Galbraith C.G. 1998. Cell migration: regulation of force on extracellular-matrix-integrin complexes. *Trends in Cell Biology* 8: 51–54.

Shih W., Gallusser A. & Kirchhausen T. 1995. A Clathrin-binding Site in the Hinge of the β2 Chain of Mammalian AP-2 Complexes. *Journal of Biological Chemistry* 270: 31083–31090.

Shin J., Kim H.N., Bhang S.H., Yoon J., Suh K., Jeon N.L. & Kim B. 2017. Topography-Guided Control of Local Migratory Behaviors and Protein Expression of Cancer Cells. *Advanced Healthcare Materials* 6.

Smilenov L.B., Mikhailov A., Pelham R.J., Marcantonio E.E. & Gundersen G.G. 1999. Focal Adhesion Motility Revealed in Stationary Fibroblasts. *Science* 286: 1172–1174.

Sochacki K.A. & Taraska J.W. 2019. From Flat to Curved Clathrin: Controlling a Plastic Ratchet. *Trends in Cell Biology* 29: 241–256.

Sperry R.W. 1963. Chemoaffinity in the orderly growth of nerve fiber patterns and connections. *Proceedings of the National Academy of Sciences* 50: 703–710.

Stoker M., O'Neill C., Berryman S. & Waxman V. 1968. Anchorage and growth regulation in normal and virus-transformed cells. *International Journal of Cancer* 3: 683–693.

Stoker M.G.P. & Rubin H. 1967. Density Dependent Inhibition of Cell Growth in Culture. *Nature* 215: 171–172.

Sun B. 2021. The mechanics of fibrillar collagen extracellular matrix. *Cell Reports Physical Science* 2: 100515.

Szent-Györgyi A. 1942. The reversibility of the contraction of myosin threads. *Studies from the Institute of Medical Chemistry, University of Szeged* 2: 25–26.

Takeichi M. 1977. Functional correlation between cell adhesive properties and some cell surface proteins. *The Journal of cell biology* 75: 464–474.

Tamkun J.W., DeSimone D.W., Fonda D., Patel R.S., Buck C., Horwitz A.F. & Hynes R.O. 1986. Structure of integrin, a glycoprotein involved in the transmembrane linkage between fibronectin and actin. *Cell* 46: 271–282.

Théry M., Jiménez-Dalmaroni A., Racine V., Bornens M. & Jülicher F. 2007. Experimental and theoretical study of mitotic spindle orientation. *Nature* 447: 493–496.

Théry M., Racine V., Pépin A., Piel M., Chen Y., Sibarita J.-B. & Bornens M. 2005. The extracellular matrix guides the orientation of the cell division axis. *Nature Cell Biology* 7: 947–953.

Thiery J.P., Brackenbury R., Rutishauser U. & Edelman G.M. 1977. Adhesion among neural cells of the chick embryo. II. Purification and characterization of a cell adhesion molecule from neural retina. *Journal of Biological Chemistry* 252: 6841–6845.

Usukura E., Narita A., Yagi A., Ito S. & Usukura J. 2016. An Unroofing Method to Observe the Cytoskeleton Directly at Molecular Resolution Using Atomic Force Microscopy. *Scientific Reports* 6: 27472.

Wehrle-Haller B. 2012. Structure and function of focal adhesions. *Current Opinion in Cell Biology* 24: 116–124.

Wood K.M. & Smith C.J. 2021. Clathrin: The molecular shape shifter. *Biochemical Journal* 478: 3099–3123.

Worth D.C. & Parsons M. 2010. Advances in imaging cell–matrix adhesions. *Journal of Cell Science* 123: 3629–3638.

Yamaguchi N. & Knaut H. 2022. Focal adhesion-mediated cell anchoring and migration: from *in vitro* to *in vivo*. *Development* 149.

Yennek S., Burute M., Théry M. & Tajbakhsh S. 2014. Cell Adhesion Geometry Regulates Non-Random DNA Segregation and Asymmetric Cell Fates in Mouse Skeletal Muscle Stem Cells. *Cell Reports* 7: 961–970.

Yoshida C. & Takeichi M. 1982. Teratocarcinoma cell adhesion: Identification of a cell-surface protein involved in calcium-dependent cell aggregation. *Cell* 28: 217–224.

Yu C., Rafiq N.B.M., Cao F., Zhou Y., Krishnasamy A., Biswas K.H., Ravasio A., Chen Z., Wang Y.-H., Kawauchi K., Jones G.E. & Sheetz M.P. 2015. Integrin-beta3 clusters recruit clathrin-mediated endocytic machinery in the absence of traction force. *Nature Communications* 6: 8672.

Zaidel-Bar R., Cohen M., Addadi L. & Geiger B. 2004. Hierarchical assembly of cell–matrix adhesion complexes. *Biochemical Society Transactions* 32: 416–420.

Zaidel-Bar R., Itzkovitz S., Ma'ayan A., Iyengar R. & Geiger B. 2007. Functional atlas of the integrin adhesome. *Nature Cell Biology* 9: 858–867.

Zamir E., Katz B.-Z., Aota S., Yamada K.M., Geiger B. & Kam Z. 1999. Molecular diversity of cell-matrix adhesions. *Journal of Cell Science* 112: 1655–1669.

Zhang X., Jiang G., Cai Y., Monkley S.J., Critchley D.R. & Sheetz M.P. 2008. Talin depletion reveals independence of initial cell spreading from integrin activation and traction. *Nature Cell Biology* 10: 1062–1068.

Zhang W., Lu C.-H., Nakamoto M.L., Tsai C.-T., Roy A.R., Lee C.E., Yang Y., Jahed Z., Li X. & Cui B. 2023. Curved adhesions mediate cell attachment to soft matrix fibres in three dimensions. *Nature Cell Biology* 25: 1453–1464.

Zielinski R., Mihai C., Kniss D. & Ghadiali S.N. 2013. Finite Element Analysis of Traction Force Microscopy: Influence of Cell Mechanics, Adhesion, and Morphology. *Journal of Biomechanical Engineering* 135.

Zuidema A., Wang W., Kreft M., Bleijerveld O.B., Hoekman L., Aretz J., Böttcher R.T., Fässler R. & Sonnenberg A. 2022. Molecular determinants of αVβ5 localization in flat clathrin lattices – role of αVβ5 in cell adhesion and proliferation. *Journal of Cell Science* 135.

Zuidema A., Wang W., Kreft M., Molder L. te, Hoekman L., Bleijerveld O.B., Nahidiazar L., Janssen H. & Sonnenberg A. 2018. Mechanisms of integrin αVβ5 clustering in flat clathrin lattices. *Journal of Cell Science*.

Zuidema A., Wang W. & Sonnenberg A. 2020. Crosstalk between Cell Adhesion Complexes in Regulation of Mechanotransduction. *BioEssays* 42.

APPENDIX 1. LIST OF ANTIBODIES UTILIZED IN IMMUNOFLUORESCENCE STAINING

Primary Antibodies					
Antigen	**Species specificity**	**Host**	**Clonality**	**Provider**	**Catalog number**
Tensin1	Human	Rabbit	Polyclonal	Sigma	SAB4200283
FAK (H-1)	Human	Mouse	Monoclonal	SantaCruz	SC-1688
p-FAK Y397	Human	Rabbit	Polyclonal	Invitrogen	44-624G
Talin1 (8D4)	Human	Mouse polyclonal	Polyclonal	Sigma	T3287
Vinculin (H-10)	Human	Mouse	Monoclonal	SantaCruz	SC-25336
p-Paxillin y118 (E9U9)	Human	Rabbit	monoclonal	cell signaling	69363
Numb	Human	Goat	Polyclonal	Invitrogen	PA1-32452

Secondary Antibodies					
Antigen	**Host**	**Clonality**	**Conjugation**	**Provider**	**Catalog number**
Rabbit Immunoglobulin G (Heavy and Light chains)	Goat	Polyclonal	AlexaFluor 488	Jackson Immuno research	111-545-003
Mouse Immunoglobulin G (Heavy and Light chains)	Goat	Poly clonal	AlexaFluor 488	Jackson Immuno research	115-545-003
Goat Immunoglobulin G (Heavy and Light chains)	Goat	Polyclonal	AlexaFluor 647	Jackson Immuno research	705-605-003

APPENDIX 2. DONOR TEMPLATE SEQUENCES

U2Os-ITGB5-mScarlet cell line:

5′-GGTTTGAGTGTGTGAGCTAACATGTGTCCTCATCCTCTTCCCCGCCGT
GTTCTGTAGGCTTCAAATCCATTATACAGAAAGCCTATCTCCACGCAC
ACTGTGGACTTCACCTTCAACAAGTTCAACAAATC**A**TA**T**TAA**C**GGCACT
GT**T**GAC**GGAAGTGCATCTGGGAGCTCAGGCGCTAGTGGTTCAGCG**
AGCGGG*GTGAGCAAGGGCGAGGCAGTGATCAAGGAGTTCATGCGGTTC*

AAGGTGCACATGGAGGGCTCCATGAACGGCCACGAGTTCGAGATCGAGGGC
GAGGGCGAGGGCCGCCCCTACGAGGGCACCCAGACCGCCAAGCTGAAG
GTGACCAAGGGTGGCCCCCTGCCCTTCTCCTGGGACATCCTGTCCCCTCAG
TTCATGTACGGCTCCAGGGCCTTCATCAAGCACCCCGCCGACATCCCCGAC
TACTATAAGCAGTCCTTCCCCGAGGGCTTCAAGTGGGAGCGCGTGATGAAC
TTCGAGGACGGCGGCGCCGTGACCGTGACCCAGGACACCTCCCTGGAGGAC
GGCACCCTGATCTACAAGGTGAAGCTCCGCGGCACCAACTTCCCTCCTGAC
GGCCCCGTAATGCAGAAGAAGACAATGGGCTGGGAAGCATCCACCGAG
CGGTTGTACCCCGAGGACGGCGTGCTGAAGGGCGACATTAAGATGGCCCTG
CGCCTGAAGGACGGCGGCCGCTACCTGGCGGACTTCAAGACCACCTACAAG
GCCAAGAAGCCCGTGCAGATGCCCGGCGCCTACAACGTCGACCGCAAGTTG
GACATCACCTCCCACAACGAGGACTACACCGTGGTGGAACAGTACGAACGC
*TCCGAGGGCCGCCACTCCACCGGCGGCATGGACGAGCTGTACAAG*TAATGT
TTCCTTCTCCGAGGGGCTGGAGCGGGGATCTGATGAAAAGGTCAGACT
GAAACGCCTTGCACGGCTGCTCGGCTTGATCACAGCTCCCTAGGTAGG
CACCACAGAGAAGACCTTCTAGTGAGCCTGGGCCAGGAGCCCACAGTG
CCT-3′, where **A** = silent mutations in 5′ homology arm, flexible linker region (GSASGSSGASGSASG) is **bold**, and mScarlet is *italic*.

U2Os-AP2-halo cell line:

5′-*GGCCAGCATCCTGGGGGGCCTCGTCTCACCCCAGGGTCTCCCCTCACA*
CAGGTTTACACGGTCGTGGACGAGATGTTCCTGGCTGGCGAAATCCGAGAG
ACCAGCCAGACGAAGGTGCTGAAACAGCTGCTGATGCTACAGTCCCTG
*GAG***GGAAGTGCATCTGGGAGCTCAGGCGCTAGTGGTTCAGCGAGC**
GGGGCAGAAATCGGTACTGGCTTTCCATTCGACCCCCATTATGTGGAA
GTCCTGGGCGAGCGCATGCACTACGTCGATGTTGGTCCGCGCGATGGC
ACCCCTGTGCTGTTCCTGCACGGTAACCCGACCTCCTCCTACGTGTGG
CGCAACATCATCCCGCATGTTGCACCGACCCATCGCTGCATTGCTCCA
GACCTGATCGGTATGGGCAAATCCGACAAACCAGACCTGGGTTATTTC
TTCGACGACCACGTCCGCTTCATGGATGCCTTCATCGAAGCCCTGGGT
CTGGAAGAGGTCGTCCTGGTCATTCACGACTGGGGCTCCGCTCTGGGT
TTCCACTGGGCCAAGCGCAATCCAGAGCGCGTCAAAGGTATTGCATTT
ATGGAGTTCATCCGCCCTATCCCGACCTGGGACGAATGGCCAGAATTT
GCCCGCGAGACCTTCCAGGCCTTCCGCACCACCGACGTCGGCCGCAAG
CTGATCATCGATCAGAACGTTTTTATCGAGGGTACGCTGCCGATGGGT
GTCGTCCGCCCGCTGACTGAAGTCGAGATGGACCATTACCGCGAGCCG
TTCCTGAATCCTGTTGACCGCGAGCCACTGTGGCGCTTCCCAAACGAG
CTGCCAATCGCCGGTGAGCCAGCGAACATCGTCGCGCTGGTCGAAGAA
TACATGGACTGGCTGCACCAGTCCCCTGTCCCGAAGCTGCTGTTCTGG
GGCACCCCAGGCGTTCTGATCCCACCGGCCGAAGCCGCTCGCCTGGCC
AAAAGCCTGCCTAACTGCAAGGCTGTGGACATCGGCCCGGGTCTGAAT
CTGCTGCAAGAAGACAACCCGGACCTGATCGGCAGCGAGATCGCGCGC
TGGCTGTCGACGCTCGAGATTTCCGGCTGA*GGGCAGGCGAGCCCCACC*

CCGGCCCCGGCCCCTCCTGGACTCGCCTGCTCGCTTCCCCTTCCCAGGCCC
GTGGCCAACCCAGCAGTCCTTCCCTCAGCTGCCTAGGAGGAAGGGACCCAG
CTGGGTCTGGGCCACAAGGGAGGAGACTGC-3'

In the construct, codon-optimized C-terminal tagging with HaloTag is underlined, while the flexible linker region (GSASGSSGASGSASG) is emphasized in bold. Additionally, *italicized* 150-bp homology arms were integrated through PCR amplification from a synthesized, codon-optimized monomeric HaloTag.